Application of Non-Orthogonal Multiple Access for Machine Type Communication in Terahertz Band

Journal:	*IEEE Access*
Manuscript ID	Access-2019-65469
Manuscript Type:	Regular Manuscript
Date Submitted by the Author:	29-Dec-2019
Complete List of Authors:	KHAN, A M MUSA SHAKIB; BRAC University, EEE Sabuj, Saifur; Hanbat National University, Electronices and Control Englinnering Hamamura, Masanori; Kochi University of Technology,
Keywords: Please choose keywords carefully as they help us find the most suitable Editor to review:	4G mobile communication, Wireless communication, Communication networks
Subject Category Please select at least two subject categories that best reflect the scope of your manuscript:	Communications technology, Information theory
Additional Manuscript Keywords:	machine-to-machine communication, non-orthogonal multiple access, terahertz

IEEE Access
Multidisciplinary | Rapid Review | Open Access Journal

Date of publication xxxx 00, 0000, date of current version xxxx 00, 0000.

Digital Object Identifier 10.1109/ACCESS.2017.DOI

Application of Non-Orthogonal Multiple Access for Machine Type Communication in Terahertz Band

A M MUSA SHAKIB KHAN[1], SAIFUR RAHMAN SABUJ[2], (MEMBER, IEEE), AND MASANORI HAMAMURA.[3], (Member, IEEE)

[1]Department of Electrical and Electronic Engineering, Brac University, Bangladesh (e-mail: a.m.musa.shakib.khan@g.bracu.ac.bd)
[2]Department of Electronics and Control Engineering, Hanbat National University, South Korea (e-mail: s.r.sabuj@ieee.org)
[3]Graduate School of Engineering, Kochi University of Technology, Japan (e-mail: hamamura.masanori@kochi-tech.ac.jp)

Corresponding author: Saifur Rahman Sabuj (e-mail: s.r.sabuj@ieee.org).

ABSTRACT There is a compelling need to address the problem of accommodating the rapidly growing number of machine type devices engaging in communication within the scarce radio spectrum, in current and forthcoming generations of wireless networks. The coming decades will also witness various novel applications, demanding wireless communication at very high data rate and energy efficiency, which currently favored technologies and techniques are inadequate to support. Because of these reasons, it seems inevitable that wireless communication will have to be facilitated by the efficient utilization of larger bandwidth at higher frequencies. Non-Orthogonal Multiple Access (NOMA) and shifting to higher frequency ranges such as the lower terahertz band, have been considered as solutions to provide space to the increasing number of communicating devices while meeting performance requirements. In this paper a machine type communication system model, utilizing the promising technique NOMA and operating in the lower terahertz band, is developed and analyzed for its performances of data rate and energy efficiency. The use of NOMA in the terahertz band is justified by referring to previous works on each of these techniques as well as by the results of simulations and comparisons with NOMA implemented in the mmWave band. Thereafter the energy efficiency of the proposed model is maximized by using unconstrained optimization and then constrained (by threshold of data rate) optimization, the latter solving a multi-objective problem by the ϵ-constraint method. The optimal transmission power is also derived for both optimization techniques. Finally, simulation results demonstrate that the best case scenario for energy efficiency can be achieved by utilizing unconstrained optimization for machine-to-machine communications and constrained optimization for base-to-machine communications.

INDEX TERMS Data rate, energy efficiency, machine-to-machine communication, mmWave, non-orthogonal multiple access, optimization technique and terahertz.

I. INTRODUCTION

AS an exponentially growing number of devices are participating in the Internet of Things (IoT), its impact on individuals, businesses, economies and societies is going to be massive. With estimations of a trillion sensors and billions of users to be connected to the Internet by the year 2021 [1], wireless data traffic, a crucial facilitator of IoT, is thus expected to increase in several folds by 2021. Furthermore, we are witnessing the advent of applications such as virtual and augmented reality, self driving cars, telesurgery, wireless backhaul, etc. In fact, within the next decade there could be even newer applications not envisioned yet. Almost all of these applications will have stringent requirements of low latency, high data rate, spectral and energy efficiency, at a level greater than even fifth generation (5G) networks can provide [2].

Given such a scenario, there is urgency for suitably accommodating users and sensors within the available yet limited frequency spectrum in order to enable the required level of communication. Various technologies and techniques are being investigated to prevent wireless spectrum saturation, e.g., by shifting to higher frequency ranges to obtain required bandwidths or using more efficient means of utilizing the already available frequencies. In [2], Rappaport et al. explain

that required data rates such as those in the order of 100 Gigabits per second may only be available at frequencies beyond the 100 GHz mark.

The frequency spectrum between 100 GHz and 10 THz is identified as the Terahertz (THz) band. Its feasibility of accommodating the increasing number of wireless communication devices and supporting the new applications, is currently being examined. Along with providing vastly greater bandwidth and data rate support, operating in this band is advantageous in terms of robustness in various unfavorable environments, resisting noise from optical sources, supporting strong communication security, etc. without posing any health concern [3]. One of the major drawbacks of the technology, however, is that operating in frequencies above 1 THz results in considerable propagation losses, thus severely limiting the range of communication. Considering how operating in the lower THz bands has enabled covering a reasonable range of distance [4], this paper has carried out analysis in the lower part of this spectrum.

In order to combat spectral saturation, which is a hindrance to the requirements of massive connectivity, researchers have recently demonstrated their interest in non orthogonal multiple access (NOMA). Multiple access (MA) techniques can be broadly classified into orthogonal multiple access (OMA) and NOMA. Although, OMA has been utilized in the present and earlier generations of networks, currently there is consensus that NOMA is essential, and potentially more effective than OMA for the applications and requirements of 5G networks and beyond. NOMA brings better spectral efficiency and throughput to communicating systems than OMA, by assigning the same frequency to multiple users (hence non-orthogonal) while segregating in the power or code domain, thus enabling massive connectivity through the share of communication resources. Furthermore, it also provides better user fairness, lower latency and compatibility with present and upcoming systems of communication [5]. NOMA is not a fundamentally novel technique: from an information theory perspective, the idea of sharing communication resources non orthogonally was understood previously as well. However, despite its potentials over OMA, NOMA implementation was held back primarily due to the level of signal processing and associated processing power required by receivers. For NOMA receivers to discern and detect their anticipated signals from a superposition of various others which reach them, they need to be complex enough to carry out successive interference cancellation (SIC). However, that level of complexity for receivers was deemed unacceptable in the previous generations. Today, with advances in processing power capabilities, there has been a reconsideration of SIC and hence NOMA within the research fields of both academia and industry [6]. Because the migration to higher frequency spectra within the near future seems inevitable, and NOMA appears to be the ideal MA technique, this paper investigates the use of NOMA in the lower THz band, in order to effectively and efficiently utilize the bandwidth in this domain. This establishes the rationale for investigating the integration of these two technologies.

As well as using NOMA, this paper also makes use of orthogonal frequency division multiplexing (OFDM), a multicarrier modulation technique that forms the basis of MA in 4G and LTE systems. OFDM's working principle is to divide the available bandwidth or resource blocks into a number of narrow band, overlapping but orthogonal subcarriers (SCs). OFDM techniques have been used in IoT networks such as downlink Narrow Band IoT (NB-IoT): a standard presented by 3GPP and designed for massive numbers of machine type communication (MTC) devices over long ranges, low rate and energy efficient links. Using narrow bandwidths, the NB-IoT standard has greater coverage than global positioning system/general packet radio service and is also able to filter out relatively more noise, thus yielding better signal to interference and noise ratio (SINR) [7]. In order to investigate how each of the above mentioned technologies integrate, our system model runs over a narrow band in the THz spectrum, utilizing OFDM as well as power domain NOMA to enable each of the OFDM SCs to be shared by multiple devices, segregated by their transmission power levels. Such a communication system should theoretically support a vast number of devices and higher levels of spectral efficiency, than what could have been supported by OFDM systems alone, which allows each SC to be occupied by only one device per time slot [8].

Machine to machine communication is an integral part of the IoT landscape, where various types of sensors and devices independently communicate among themselves, sharing information and collaborating on projects, without being governed centrally. Information that is gathered by these devices are often passed onto actuators in real time control systems. Therefore, the ability to guarantee high levels of reliability and timing may be critical for many such devices. Based on this criterion, two classes of machine type communication devices (MTCDs) exist: (i) ultra reliable low latency communication (URLLC) devices, characterized also by high communication power requirements and (ii) massive machine type communication (mMTC) devices, characterized by much lower cost, power and moderate latency and reliability requirements. The former class of devices is going to be utilized in applications such as autonomous driving, telesurgery and industry automation while the latter class will be functional as metering, monitoring and sensing devices [9]. This paper presents a system model of a wireless network of MTCDs, evaluated for its performance in the downlink scenario, using the aforementioned techniques of NOMA over OFDM SCs in the lower THz band. Hence, the main contributions of this paper are:

- Establishing a case for utilization of NOMA in the lower THz band.
- Proposing a novel system model where four MTCDs utilize NOMA to share one OFDM SC over a narrow, lower THz band of frequency. This is one of the first investigations of NOMA in the THz band and attempts to enable massive connectivity of devices with enhanced

communication performance.
- Derivation of data rate and energy efficiency for various communication links of the proposed model.
- Maximizing energy efficiency of the proposed model, first via unconstrained optimization and then via constrained optimization by formulating a multi-objective problem and solving it with the ϵ-constraint method.
- Highlighting energy efficiency performance of the MTCDs between themselves, observing its maximization with the optimization techniques used and comparing between the techniques.

The organization of the paper henceforth is as follows. Section II discusses related works to this study, section III presents and explains the system model, along with equations of SINR, channel gain, data rate, energy efficiency and optimization techniques for maximum energy efficiency, section IV consists of the results from numerical simulations and discussions of the plots and finally section V concludes the paper with the best scheme for energy efficiency of proposed model and suggestions for future studies.

II. RELATED WORKS

In this section, some of the major works related to the techniques and schemes are briefly highlighted.

In order to unify the existing knowledge on Terahertz communication research, [4] made a comprehensive overview of the technology, highlighting its potential benefits (such as terabit-per-second capacities of communication, smaller transceivers and improved energy efficiency) and the important research challenges to be addressed (e.g., barriers to designing THz electronics and media access control mechanisms, modelling THz communication channels, coverage and deployment strategies, etc.). Furthermore, use cases of the technology and design and performance trade-offs were also discussed. In a more recent literature [3], another review of THz technology was made. The authors cited newer research performed to develop THz channel models, mentioning how one particular study was the first to present single sweep THz measurements which could help in the design of THz transceiver electronics. The paper also mentioned some more use cases of THz technology such as hybrid THz-optical wireless links using THz to assist unmanned air vehicles communication in data centers, heterogeneous mobile networks and 3D beamforming.

With regards to NOMA, its power domain version was put forward as a technology for Future Radio Access (FRA) in [5], along with Successive Interference Cancellation (SIC) for decoding, and shown to exhibit improved capacity and cell-edge throughput performance, without frequency selective channel quality indicator being necessarily available at the base station (BS). In [10], NOMA in a multiple input single output (MIMO) broadcast scenario, with the use of Lagrange method and Newton's iterative algorithms to derive minimum transmission powers (also for certain special cases) and optimum precoding vectors, was found to have competitive performance when compared with performance using the optimal strategy of dirty paper coding. The study presented in [11], summarized NOMA as a concept, differentiated between its types and developments such as single carrier, multi-carrier, MIMO-NOMA, cooperative NOMA, millimeter-wave NOMA, issues with practical implementation and major challenges as of the time of the research.

Due to the requirements of better energy efficiency levels in the wireless communication domain, different algorithms have been used to investigate the performance of various system models of NOMA. In [12], the research in energy efficient resource allocation problem for NOMA was done for the first time. Using simulations, the authors demonstrated the superior energy efficiency and capacity of downlink NOMA over OFDMA systems using their suggested algorithms, which incorporated schemes for assigning subchannels and allocating power between users. Further work on solving NOMA user scheduling and power allocation problems have been done in [13], this time in the context of post-LTE heterogeneous networks by taking into account different levels of channel state information (CSI). Following the application of convex optimization on these areas, the researchers produced schemes to improve NOMA performance, made comparisons with techniques existing till then and concluded that energy efficiency performance of NOMA systems could be improved with effective user scheduling and power allocation schemes. In [14], some of the authors of [12] furthered their previous work by regarding energy efficiency, power availability, quality-of-service, etc., in downlink NOMA. They analyzed their system model for its subchannel and power assignments, using algorithms (founded on matching theory) and Lyapunov optimization with constraints, respectively. In another paper [15], to maximize energy efficiency in a downlink MIMO-NOMA scenario, the authors attempted to optimize user scheduling by applying methods based on signal space alignment (SSA) to reduce complexity and signaling overhead together with aiming to develop an energy efficient power allocation scheme based on sequential convex approximation (SCA).

A number of recent literature demonstrated the excellence of MIMO-NOMA over MIMO-OMA. For example, MIMO-NOMA was shown to have better sum channel capacity, ergodic sum capacity and user fairness than MIMO-OMA in [16], [17]. In [18], the authors provide a divide-and-next-largest-difference-based user pairing algorithm for downlink MIMO-NOMA to ascertain fairness in terms of sum rate gain and then makes a comparison between MIMO-NOMA and MIMO-OMA, to again find the superiority of the former over the latter in terms of outage probability and effective sum rate.

Regarding NB-IoT, the study [19] provided a detailed review of the technology starting from its development history, standardization, its functionality, innovations on the technology, its performances when compared with other LPWAN technologies and applications of NB-IoT. Authors concluded by pointing out the security issues of NB-IoT which need to be attended. An interesting and recent literature [8], pre-

TABLE 1. Related schemes and techniques in NOMA

Reference	Summaries of papers utilizing NOMA	Optimization Technique/Algorithm utilized
[10]	QoS optimization by minimizing transmission power and by deriving optimal precoding vectors.	Lagrange dual problem and Newton's iterative method respectively.
[12]	Optimizing energy efficiency in downlink context through formulation of subchannel and power allocation problem.	Difference of convex programming.
[13]	User scheduling and power allocation in 5G heterogeneous networks considering CSI to improve energy efficiency.	Convex optimization.
[14]	Subchannel resource assignment and power allocation problem, considering energy efficiency, power availability, QoS requirements, etc.	Lyapunov optimization to divide problem into linear and Lagrangian subproblems.
[15]	User scheduling and power allocation of a MIMO-NOMA system are optimized to improve energy efficiency.	SSA method to enhance user scheduling (considering maximum collinearity between users) and SCA method, devolving into convex optimization, to form efficient power allocation scheme.
[16], [17]	Superiority of MIMO-NOMA over MIMO-OMA in terms of sum channel capacity, ergodic sum capacity and user fairness.	Optimized user admission scheme for sum rate and number of users based on SINR threshold.
[18]	Control sum rate gain between NOMA clusters and ensure fairness; show MIMO-NOMA has better outage probability and effective sum rate than MIMO-OMA.	D-NLUPA (divide and next largest difference based user pairing algorithm).
This paper	Downlink scenario, in lower THz, optimized for energy efficiency by deriving optimal transmission power, via unconstrained and constrained techniques.	Formulating single-objective problem via unconstrained optimization and multi-objective problem via constrained optimization then using ϵ-constraint method to simplify into single-optimization problem and solved using Lagrangian function.

sented a power domain NOMA mechanism for MTC in NB-IoT networks. With the aid of such strategy, along with providing algorithms to solve a combined subcarrier and transmission power assignment problem, the authors were able to maximize the total machine type communicating devices that the network could support. Our paper drew inspiration from the ideas presented by the aforementioned work.

III. SYSTEM MODEL

Consider a landscape with a BS and several MTCDs, where machine-to-machine communication (between two MTCDs) and base-to-machine communication (downlink, from BS to MTCD) is shown in Fig. 1. These MTCD (mMTC and uRLLC) communications are designed to occur over a wireless network operating within a band in the lower THz spectrum which is in turn divided into numerous resource blocks. Implementing a model in the THz band is challenging because of its peculiarity: even though higher frequencies enable acquiring of greater bandwidth, which could lead to better communication performance, they also lead to significant path loss that diminishes performance. This calls for the careful selection of a spectrum for our model that not only meets the accepted definition of the THz band but also enables an appreciable level of communication performance. Hence, calculations for determining the bandwidth of this resource block are considered $BW = f_U - f_L = (0.39 - 0.09)$ THz $= 300$ GHz.

For a large resource block of bandwidth 20 MHz, LTE physical layer standard uses OFDM to raise 1201 SCs [20]. In this paper the principle of OFDM is used to raise 1201 SC frequencies from each of 400 resource blocks, each SC with a bandwidth of approximately 500 KHz. Whereas OFDMA in LTE networks today assigns one SC to only one MTCD for communication [8], in our model, NOMA would act on top of OFDMA and enable each SC to be shared by multiple MTCDs as well as the BS, by multiplexing all these devices in the power domain. Using one same SC, a pair of mMTC devices can communicate between themselves while simultaneously a pair of URLLC devices can also communicate between themselves. Moreover, each of these four devices (MTCDs) can individually receive signals from the BS using that same SC. This can be arranged by allocating the URLLC pair with higher transmission power for communication than the mMTC pair, thus segregating the two types of devices using the same SC in the power domain. It is noted that communication is not enabled between a URLLC device and an mMTC device due to their different orders of latency. Also, in this model, the BS addresses each MTCD of a particular type in different time slots but can transmit to an mMTC and a URLLC at the same time. For the rest of the paper, the communication between MTCDs is going to be denoted as "machine-to-machine (M2M)" and the communication between MTCD and the BS as "base-to-machine (B2M)" .

For convenience of evaluating performance some constraints placed on our model are:

1) It is assumed that for a SC, each of the two URLLC devices is at a uniform distance from each mMTC device and similarly each mMTC device is also uniformly spaced from each URLLC device. Otherwise if they are placed at random distances, the channel gains would be different for every device and each would require its own measure of performance, making generalized comparisons of performances complex.
2) The BS transmits to mMTC devices at the same signal power level that the mMTC devices use to communicate with the BS and/or each other. The same applies for URLLC devices. Thus, the transmission power

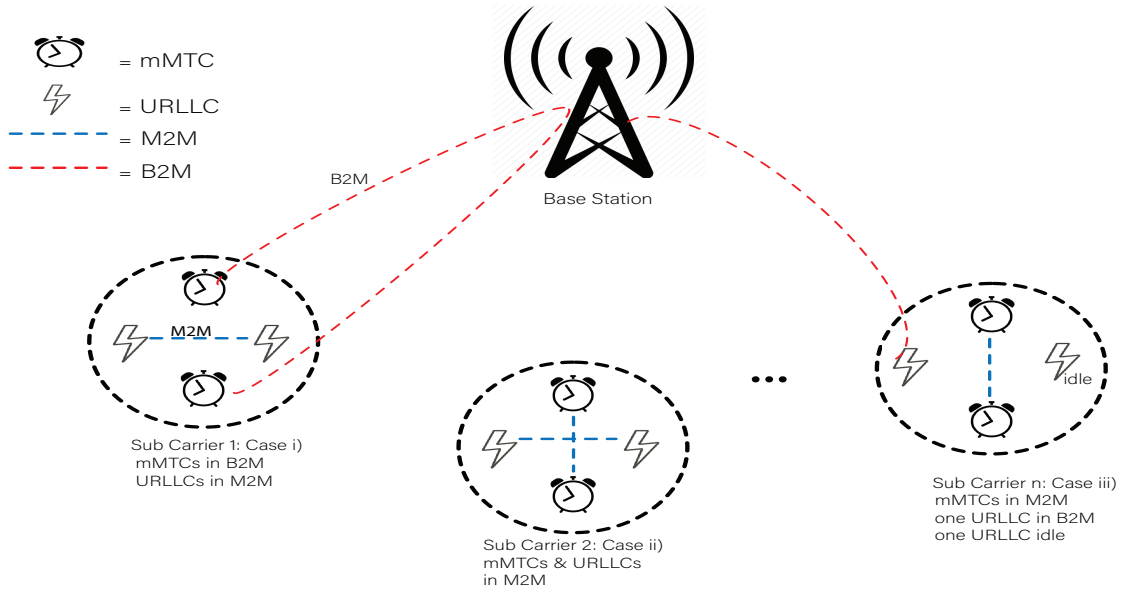

FIGURE 1. Communication links between the MTCDs and the BS.

from the BS to any MTCD and from that MTCD to the BS and the transmission power between MTCDs are all at the same level.

A. SINR WITHIN NOMA SCHEME

With the above constraints in place, we analyze the communication within a particular SC in a downlink context (i.e. in B2M mode, MTCDs are receiving from BS, without transmitting to it). At the receiver of the NOMA communication link, SIC process is performed until the receiver finds its anticipated signal. In the downlink scenario, the BS is transmitting to the MTCDs. In the ideal case, interference may only be possible for devices communicating using the same SC (since they share the same frequencies). Each receiving device needs to perform SIC to decode its own signal from that of others using the same SC. It does so by first detecting signals stronger than its own anticipated signal level, then subtracting them from the total received signal to eventually find its desired signal. Conversely, signals with power that are lower than its own are treated as noise [5].

Consider an mMTC device receiving signals from the BS or another mMTC. mMTC devices operate with signals of lower power levels than that of the lower latency URLLCs. This means that at the mMTC receivers, the arriving higher powered URLLC signals are canceled out by the SIC process and only its anticipated signals are available for decoding. As a result, URLLC devices of the same SC do not cause interference to the communication of the mMTC devices. Based on this, the generic equation of the received SINR of an mMTC device using a particular SC is given by:

$$\gamma_m = \frac{p_m |h_m|^2}{N_o B}, \tag{1}$$

where h_m, p_m, N_o and B denote the channel gain, transmission power, noise power spectral density and the SC bandwidth, respectively. Note that the channel gain changes between the M2M and B2M mode and can be denoted as $h_{m,m}$ and $h_{m,b}$, respectively. Similarly, N_o can be replaced by $N_{o,m}$ or $N_{o,b}$ to represent the different noise levels between the two modes of communication.

For a receiving URLLC device in a SC, lower power signals originating from mMTC devices and, during downlink, from the BS to the mMTC devices pose different levels of interference to the URLLC's anticipated signals. Using SIC, the receiving URLLC device is able to recognize the different power levels of signals, treating these lower power levels (to be denoted by variable "I") as noise to its anticipated level of power signal. Hence, a generalized equation for the received SINR of a URLLC device is given by:

$$\gamma_u = \frac{p_u |h_u|^2}{I + N_o B}, \tag{2}$$

where h_u, p_u, N_o, I and B denote the channel gain, transmission power, the noise power spectral density, the lower power interference and the SC bandwidth, respectively. Again, the channel gain changes between the M2M and B2M mode and can be denoted as $h_{u,u}$ and $h_{u,b}$, respectively. Similarly, N_o can be replaced by $N_{o,u}$ or $N_{o,b}$ between the two modes of communication. The term I is either I_b or I_m. I_b is represented by

$$I = I_b = n_b \cdot p_m \cdot |h_{m,b}|^2, \tag{3}$$

where $n_b = 1$ if BS is transmitting to mMTCs (B2M mode) and $|h_{m,b}|^2$ is the channel gain for the path between the mMTC device and the BS. I_m is represented by

$$I = I_m = n_m \cdot p_m \cdot |h_{m,m}|^2, \tag{4}$$

where the variable $n_m = 1$ is used to show if the mMTC devices are communicating with each other (M2M mode) and $|h_{m,m}|^2$ is the channel gain for the path between the mMTC devices. When $n_b = 1$, n_m must be "0" and vice versa. This is because when mMTC is in B2M mode, it cannot also be in M2M mode (can only communicate with another device or the BS during a particular time frame).

Thus, for the URLLC device in this system model, interference arise either from the I_b or the I_m term, depending on whether the mMTC device sharing the frequency band is in B2M or M2M mode, but not both simultaneously. Note that in the best case scenario, mMTC devices are not communicating at all and hence pose no interference, thereby maximizing SINR for URLLC devices, but we have considered the worst case scenarios here.

B. CHANNEL GAIN FROM PATH LOSS MODEL

Path loss is the attenuation of electromagnetic wave power as it propagates through space from the transmitter to the receiver. For this system model, the channel gain of the various M2M and B2M communication links are derived from the path loss models found in [21], [22]. As pointed out in section I (Introduction), THz band is an upcoming technology with several potential benefits for wireless communications. Hence, considering a carrier in the lower THz band of frequency 0.2 THz (with upper and lower cut-offs of 0.39 THz and 0.09 THz respectively), line of sight (LOS) and non line of sight (NLOS) expressions of path loss for M2M and B2M communications can be given by these expressions:

$$PL_{M2M}^{LOS} = 16.9\log_{10}(d[m]) + 78.8, \tag{5}$$
$$PL_{M2M}^{NLOS} = 40\log_{10}(R[km]) + 208, \tag{6}$$
$$PL_{B2M}^{LOS} = 22\log_{10}(d[m]) + 74, \tag{7}$$
$$PL_{B2M}^{NLOS} = 36.7\log_{10}(d[m]) + 82.6, \tag{8}$$

where d is expressed in m and R is expressed in km. Using the above, the average path loss can be expressed by the following:

$$PL(d) = \alpha \cdot PL_{LOS} + (1-\alpha) \cdot PL_{NLOS}, \tag{9}$$

where α is the probability co-efficient of LOS, PL_{LOS} is the LOS path loss and PL_{NLOS} is the NLOS path loss. For each case above, channel gain $|h|^2$ can be evaluated by the expression:

$$|h|^2 = 10^{-\frac{PL(d)}{10}}, \tag{10}$$

C. EVALUATING PERFORMANCE METRIC

In this section, we analyze the performance metric such as the data rate, energy efficiency and develop optimization techniques for the various M2M and B2M communications of our system model.

1) Data Rate

For an mMTC device, the generic equation for its attainable data rate using the expression for received SINR from equation (1) is given by the following expression:

$$R_m = B \cdot \log_2\left(1 + \frac{p_m |h_m|^2}{N_o B}\right), \tag{11}$$

where the channel gain h_m changes according to the particular mode of the device's communication: M2M or B2M, as explained previously.

Similarly, for a URLLC device, using the SINR expression from equation (2), the following expression gives its attainable data rate:

$$R_u = B \cdot \log_2\left(1 + \frac{p_u |h_u|^2}{I + N_o B}\right), \tag{12}$$

where the channel gain h_u changes according to the particular mode of the device's communication: M2M or B2M.

As explained in equations (3) and (4), the term "I" in the above equation can either be $I = I_b$ or $I = I_m$ depending on whether the mMTC device sharing the frequency band is in M2M or B2M mode.

At this point, it may be useful to produce a generic equation for the data rate of an MTCD device (mMTC or URLLC) for the purpose of evaluating the performance of the system model using some other metrics. This is possible because equations (11) and (12) have similar variables. Thus, the data rate of an MTCD can be expressed as:

$$R = B \cdot \log_2\left(1 + \frac{p_t |h|^2}{I + N_o B}\right), \tag{13}$$

where p_t is the transmission power of the MTCD, $|h|$ being the respective channel gain of the communication link and I being the interference if any (to be present only for URLLC receivers).

2) Energy Efficiency

Energy efficiency is defined as a measure of the number of bits transmitted per joule of consumed energy [23]. In this paper we find this metric by taking the ratio of the data rate to the total power consumption of transmitting devices (i.e. BS or MTCD).

$$EE = \frac{\mathbb{E}[R]}{P_{idle} + \mathbb{E}[p_t]}, \tag{14}$$

where $\mathbb{E}[\cdot]$ denotes the expectation operator, $\mathbb{E}[R]$ is expected value of the data rate from equations (11) and (12), P_{idle} the constant value of power consumed by the transmitting device's circuit and $\mathbb{E}[p_t]$ is expected transmission power.

3) Optimization I: Maximizing Energy Efficiency via Unconstrained Optimization

In this subsection, we attempt to derive the maximum energy efficiency that can be achieved, with respect to transmitting device's power (p_t), without immediately considering any

constraints, and thus not taking into account effect on other performance metrics such as data rate.

The maximum energy efficiency for M2M or B2M communications using equation (13) is represented by:

$$\max_{p_t>0} \frac{\mathbb{E}[R]}{P_{idle}+\mathbb{E}[p_t]}. \tag{15}$$

Taking the derivative of the above equation with respect to p_t, using the generic expression for the data rate of an MTCD from equation (13), the optimal transmission power for which we can attain maximum energy efficiency for M2M or B2M communications is:

$$p_t^{WOC} = \frac{I+N_oB}{|h|^2}\left(e^{1+W\left[e^{-1}\cdot\left(\frac{P_{idle}\cdot|h|^2}{I+N_oB}-1\right)\right]}-1\right), \tag{16}$$

where $W(\cdot)$ is Lambert function.

Proof: The derivation for the above is provided in Appendix A.

4) Optimization II: Maximizing Energy Efficiency via Constrained Optimization

This subsection derives the mathematical expressions for the maximum energy efficiency of our model, this time placing certain constraints on the data rate and binding it to a threshold. This technique may be useful for scenarios where the energy efficiency is required to be maximized without affecting the date rate performance.

In order to improve the energy efficiency performance, as given by equation (14), a multi-optimization problem (MOP) can be created which maximizes the numerator of the ratio (i.e. expected value of the data rate) while minimizing the denominator, i.e, the expected value of transmission power during operation, as shown below:

$$\min_{p_t} \quad \mathbb{E}[p_t] \tag{17a}$$

$$\max_{p_t} \quad \mathbb{E}[R] \tag{17b}$$

$$\text{s.t.} \quad p_t \geq p_{th}. \tag{17c}$$

Using the ϵ-constraint method [24], [25], the MOP problem above can be reduced to a single optimization problem (SOP) by minimizing one parameter while binding the others by allowable thresholds. The following conditions show the SOP problem at hand:

$$\min_{p_t} \quad \mathbb{E}[p_t] \tag{18a}$$

$$\text{s.t.} \quad \mathbb{E}[R] \geq R_{th} \tag{18b}$$

$$\text{s.t.} \quad p_t \geq p_{th}. \tag{18c}$$

Thus, the SOP problem above seeks to minimize the transmission power while binding the data rate to a threshold R_{th} and the transmission power above the threshold p_{th}. Using the Lagrangian method in equations (18a)-(18c), optimal transmission power can be expressed as

$$p_t^{WC} = \frac{I+N_oB}{|h|^2}\left[\exp\left(\frac{\ln(2)R_{th}}{B}\right)-1\right]. \tag{19}$$

Proof: The derivation for the above is provided in Appendix B.

IV. RESULTS AND DISCUSSION

Using the equations for the data rate, energy efficiency and required optimum power of the communication links that are considered in the system model, we have carried out a number of simulations to analyze performance in this section. For the numerical evaluation of above equations, we use the following parameters: $B = 500$ KHz, $N_o = -174$ dBm, $P_{idle} = 100$ W, $\alpha = 0.9$ for M2M and $\alpha = 0.1$ for B2M.

A. SIMULATIONS WITHOUT OPTIMIZATION

The plots in Figs. 2-9 have been performed using equations (11), (12) and (14). In this subsection, the distance between mMTC and mMTC, URLLC and URLLC, BS and mMTC, and BS and URLLC are considered as 100 m, 200 m, 300 m and 400 m, respectively.

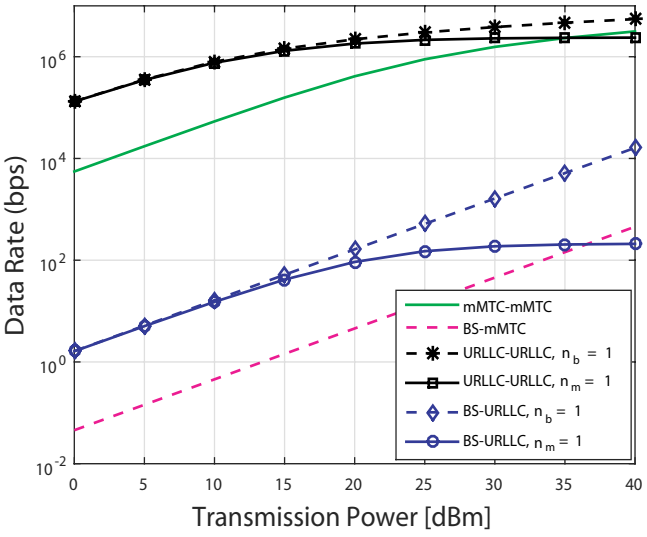

FIGURE 2. Data rate of all communication links versus transmission power in THz band.

Figure 2 shows the simulated plot of data rate versus transmission power of all the communication links discussed in this paper. Higher data rate arises for M2M communication links over B2M links, due to the relatively shorter distance in between the MTCDs in M2M mode than the larger distance between the BS and MTCDs in B2M mode. On the other hand, having greater power allocation than mMTC devices, URLLC communications achieve higher data rates. The legend shows the two cases of URLLC-URLLC links, $n_b = 1$ and $n_m = 1$. In case $n_b = 1$, URLLC-URLLC links attain higher data rate when receiving interference from the BS transmitting to mMTCs, than in case $n_m = 1$, where interference arises due to the mMTCs communicating in M2M mode. The explanation for this is that in case $n_m = 1$, the URLLC devices are nearer to the interfering mMTC transmission, while in case $n_b = 1$, the URLLC devices are farther from the interfering BS transmission. Due to fading

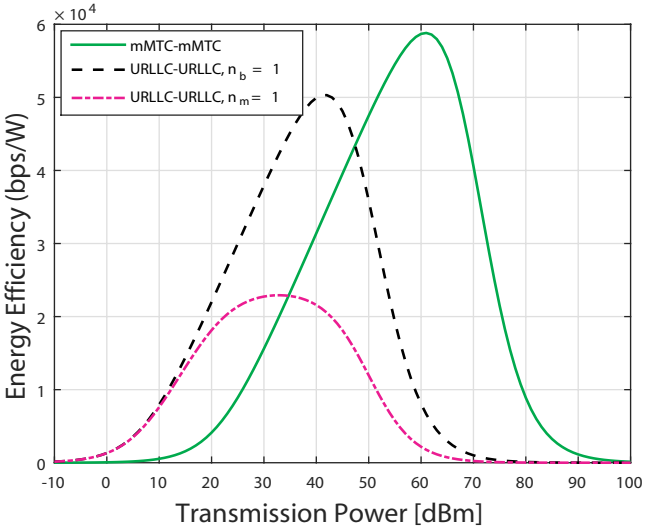

FIGURE 3. Energy efficiency of M2M communication links versus transmission power in THz band.

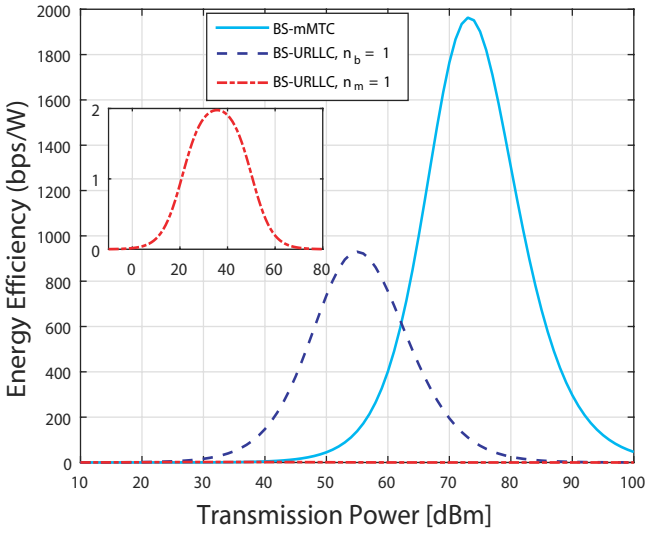

FIGURE 4. Energy efficiency of B2M communication links versus transmission power in THz band.

over longer distances, the BS-mMTC transmission thus has lower impact of interference on URLLC. This phenomenon will also be applicable for the other simulation plots in this paper. In Fig. 2, at $p_t = 25$ dBm, the data rate for the best case URLLC-URLLC ($n_b = 1$) link, at 3.00×10^6 bps, is 3.4 times higher than mMTC-mMTC at 8.90×10^5 bps. On the other hand, the best case BS-URLLC ($n_b = 1$) link at 517.1 bps has 36 times higher data rate than that of mMTC at 14.40 bps.

The plot of energy efficiency versus transmission power for M2M communication links is shown in Fig. 3. Although URLLC devices enjoy greater data rate than mMTCs, the transmission power level allocated to them is relatively much greater. As a result, the energy efficiency of mMTC devices is greater. Energy efficiency of URLLC devices for the case of $n_b = 1$ is higher than that of the case $n_m = 1$, because the data rate of the former communication link is higher than the latter. We can characterize the power for which we have peak (maximum) energy efficiency as the optimum power for these communication links with regards to energy efficiency. Thus, according to this plot, energy efficiency for mMTC-mMTC at the optimum power of 61 dBm is 5.88×10^4 bps/W, which is 14.3% higher than that of URLLC-URLLC (for case $n_b = 1$) at 5.03×10^4 bps/W for its own optimum power of 42 dBm. It is to be noted however, the required optimum power for mMTC is greater than that of URLLC.

Figure 4 shows the plot of energy efficiency versus transmission power for B2M communication links of the system model. As explained for Fig. 3, BS-mMTC link experiences greater peak energy efficiency due to power allocation for its transmission being much less than that of the BS-URLLC link. The peak energy efficiency of the BS-URLLC link for case $n_m = 1$ is justifiably the lowest, due to the lower data rate of the link (due to highest interference experienced) despite utilizing high levels of transmission power. At the

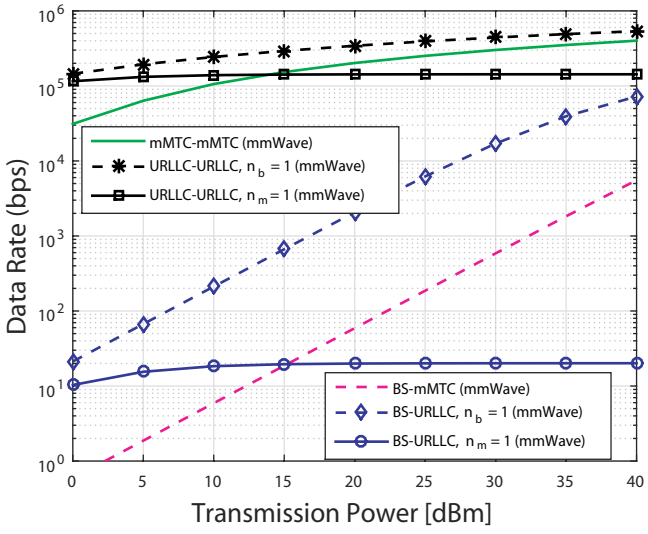

FIGURE 5. Data rate of all communication links versus transmission power in mmWave.

optimum power of 73 dBm, the BS-mMTC link has an energy efficiency of 1963 bps/W. This is 2.1 times higher than energy efficiency of BS-URLLC (case $n_b = 1$), which is 929.8 bps/W at its optimum power of 55 dBm.

An analysis of NOMA in the THz band has not been done in any previous work, as already discussed in section I (Introduction). Therefore in order to evaluate how the system model of our paper based in the lower THz band performs, a comparison with existing techniques such as operating in lower frequencies such as the mmWave band will be useful. While both 28 GHz and 73 GHz provide natural prospects for mmWave deployment [26], our simulations were carried out using the higher of these two frequencies. The path loss models used [21], [22] are as follows: $PL^{M2M}_{mmLOS} = 16.9 \log_{10}(d[m]) + 70.1$, $PL^{M2M}_{mmNLOS} =$

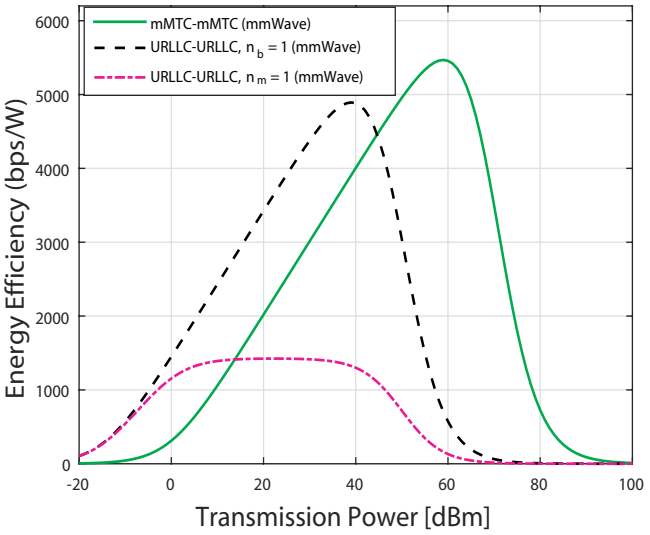

FIGURE 6. Energy efficiency of M2M communication links versus transmission power in mmWave.

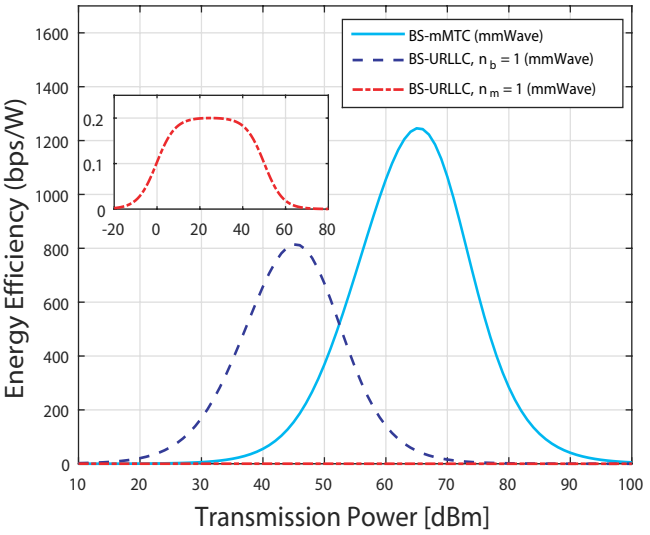

FIGURE 7. Energy efficiency of B2M communication links versus transmission power in mmWave.

TABLE 2. Comparison between the performance of NOMA in lower THz and NOMA in mmWave band.

Communication link	mmWave data rate (bps)	Lower THz data rate (bps)	Comparing data rate - operating in:	mmWave energy efficiency (bps/W)	Lower THz energy efficiency (bps/W)	Comparing energy efficiency - operating in:
mMTC-mMTC	2.52×10^5	8.90×10^5	THz is higher by 3.6 times	5468	5.88×10^4	THz is higher by 11 times
URLLC-URLLC ($n_b = 1$)	3.93×10^5	3.00×10^6	THz is higher by 7.6 times	4893	5.03×10^4	THz is higher by 10 times
BS-mMTC	186.4	14.40	mmWave is higher by 13 times	1245	1963	THz is higher by 1.6 times
BS-URLLC ($n_b = 1$)	6213	517.1	mmWave is higher by 12 times	814.4	929.8	THz is higher by 1.1 times

$40\log_{10}(d[km]) + 194.9$, $PL^{B2M}_{mmLOS} = 22\log_{10}(d[m]) + 65.3$ and $PL^{B2M}_{mmNLOS} = 36.7\log_{10}(d[m]) + 71.2$.

The bandwidth of communication in mmWave is appreciably lower than that in THz band. Theoretically, this should help communication in the THz band to reach higher data rates. At the same time, the path loss in higher frequency bands of operation is also greater, which would counteract signal transmission and hence result in lower rates of communication.

The plot of data rate versus signal transmission power of all communication links of our model based in the mmWave band is shown in Fig. 5. The overall trend or shape of the curves is similar to that of the data rate curves in the lower THz band, for the same reasons as discussed for Fig. 2. Focusing on $p_t = 25$ dBm, as we did for Fig. 2, we find that the data rate for the best case URLLC-URLLC ($n_b = 1$) link is 3.93×10^5 bps, for the mMTC-mMTC link to be 2.52×10^5 bps, for the BS-URLLC ($n_b = 1$) link to be 6213 bps and the BS-mMTC link to be 186.4 bps.

The plot of energy efficiency against transmission power is shown in Figs. 6 and 7. For M2M, the mMTC link has an energy efficiency of 5468 bps/W at optimum transmission power 59 dBm and the URLLC ($n_b = 1$) link is at 4893 bps/W for optimum power of 39 dBm. As for B2M, the mMTC link has energy efficiency of 1245 bps/W at optimum power 65 dBm and URLLC link ($n_b = 1$) has energy efficiency of 814.4 bps/W for optimum power 45 dBm.

Table 2 summarizes and draws a comparison between the performance of NOMA in lower THz and NOMA in mmWave band. According to the table, the THz band outperforms mmWave with regards to data rate for M2M communication, while for B2M communication data rate is higher in the mmWave band than in THz. The explanation for this is that at longer distances of B2M communication, the THz band signals incur significant path loss such that the data rate falls below that of mmWave communication.

In the case of energy efficiency however, THz band outperforms mmWave band for both M2M and B2M communication according to our simulations. We have therefore made the following observations from our analysis in shifting to higher frequencies such as the lower THz band from mmWave band:

- We can expect better performance in terms of energy efficiency for both short and relatively longer range communications.
- We can expect higher data rate for short range M2M

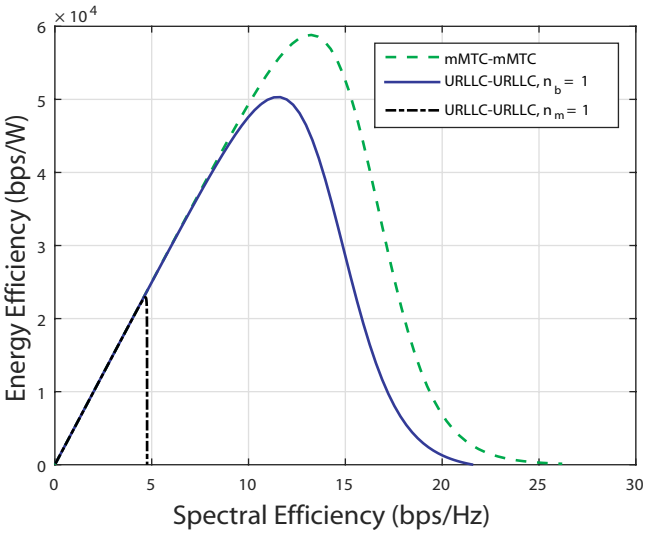

FIGURE 8. Trend of energy efficiency with spectral efficiency of M2M communication links in THz band.

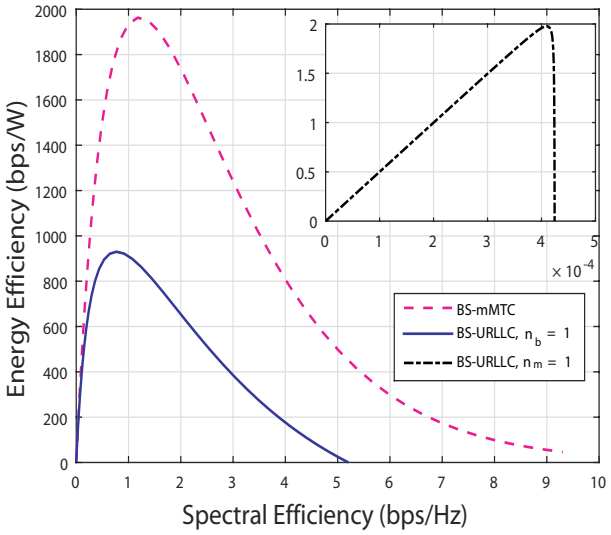

FIGURE 9. Trend of energy efficiency with spectral efficiency of B2M communication links in THz band.

communications while for longer ranged B2M communications, path loss of transmission reduces achievable data rate such that mmWave outperforms THz band operation.

These observations suggest that it may be more beneficial to implement the proposed NOMA based model in the lower THz band than in lower frequencies in order to maximize energy efficiency. Although data rate in mmWave is higher for longer distances than in lower THz, taking the factor of energy efficiency into account makes the lower THz band a better overall choice for our system model.

The plot of energy efficiency versus spectral efficiency for M2M links is shown in Fig. 8, by transmitting power from -10 dBm to 100 dBm. According to the curves, the mMTC link has peak energy efficiency of 5.882×10^4 bps/W at a higher spectral efficiency of 13.24 bps/Hz than the peak energy efficiency with a value of 5.031×10^4 bps/W, of the best case curve for URLLC link ($n_b = 1$) at its spectral efficiency of 11.64 bps/Hz. Comparing, energy efficiency and spectral efficiency of mMTC links are higher than URLLC links by 14.47% and 12.08%, respectively. According to this plot, mMTC seems to outperform URLLC with regards to energy efficiency and spectral efficiency.

Figure 9 shows the plot of energy efficiency versus spectral efficiency for B2M links, by transmitting power from -10 dBm to 100 dBm. For this case, mMTC has peak energy efficiency of 1963 bps/W, which is 2.1 times higher than peak energy efficiency of 929.8 bps/W for URLLC. In addition, spectral efficiency measurement of mMTC link is 34.68% higher (at peak energy efficiency) than spectral efficiency of best case URLLC ($n_b = 1$).

To summarize, in this subsection we observe the data rate, energy efficiency and spectral efficiency performances of our model, with the devices placed at different distances. For M2M, the best case URLLC link ($n_b = 1$) has higher data rate than mMTC communication, while although mMTC communication has potentially better energy efficiency and spectral efficiency performances, to reach these higher levels, mMTC communication requires a much higher transmission power than URLLC. On the other hand, URLLC ($n_b = 1$) communication attains peak energy efficiency using lower transmission power. As for B2M at a longer distance, mMTC outperforms URLLC with regards to data rate and potentially energy and spectral efficiency. However, as with M2M, URLLC ($n_b = 1$) achieves peak energy efficiency at lower transmission power. It seems that at longer distances, the effect of interference becomes very prominent for URLLC links and together with the factor of their high transmission power, result in lower performances in B2M. As for URLLC communication (case $n_m = 1$) witnessed much lower performances in both M2M and B2M scenarios than the other two types of link. Finally, having evaluated the proposed model in both mmWave and lower THz bands, we have determined that, in terms of data rate and energy efficiency, it might be more advantageous to operate in the latter frequencies than in the former.

B. SIMULATIONS AFTER UNCONSTRAINED OPTIMIZATION

The plots in Figs. 10-15, for unconstrained optimization, have been simulated using the equation (16) and then putting equation (16) into equations (11), (12) and (14) for data rate and energy efficiency.

The curves of required optimal transmission power versus the distance for all the communication links are shown in Figs. 10 and 11. As the distance between the communicating devices increase, the power required for transmission justifiably increases (the initial decrease for cases $n_b = 1$ is due to the factor of interference which too reduces with distance). For M2M, at distance of 100 m the optimum power required

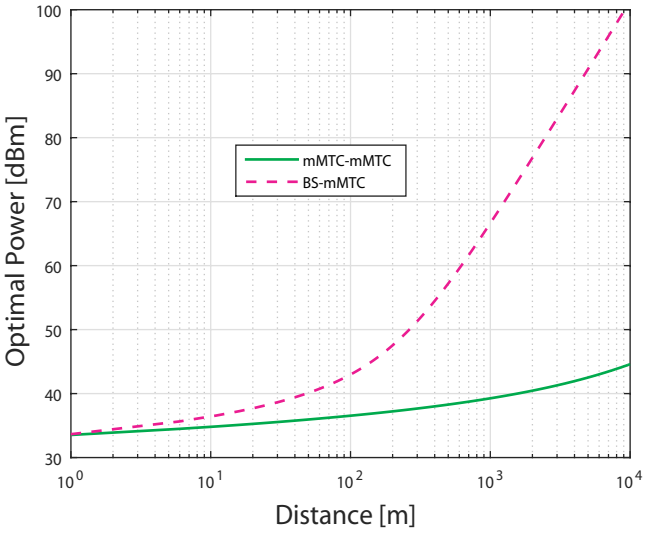

FIGURE 10. Optimal transmission power required versus distance for mMTC communication links (unconstrained optimization) in THz band.

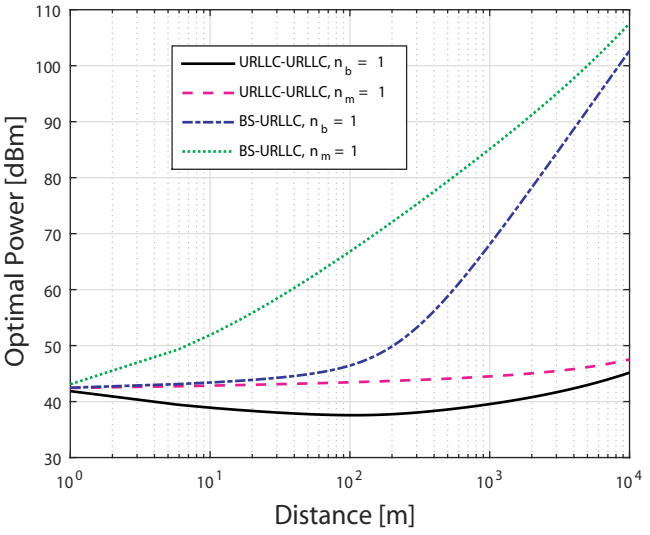

FIGURE 11. Optimal transmission power required versus distance for URLLC communication links (unconstrained optimization) in THz band.

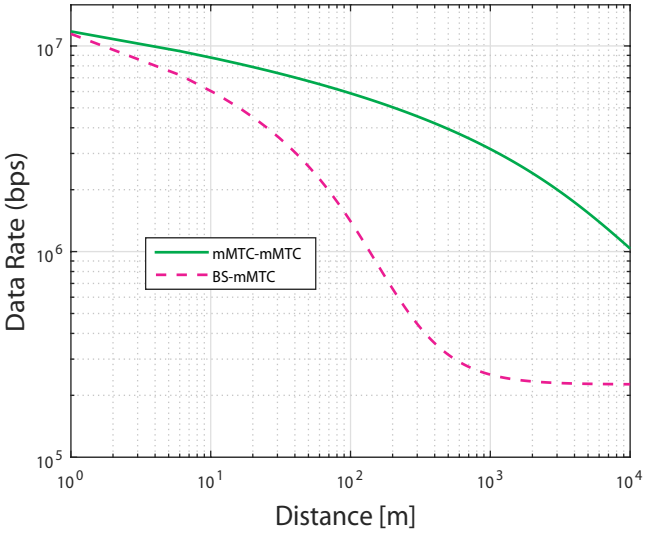

FIGURE 12. Data rate versus distance for mMTC communications, using optimal transmission power (unconstrained optimization) in THz band.

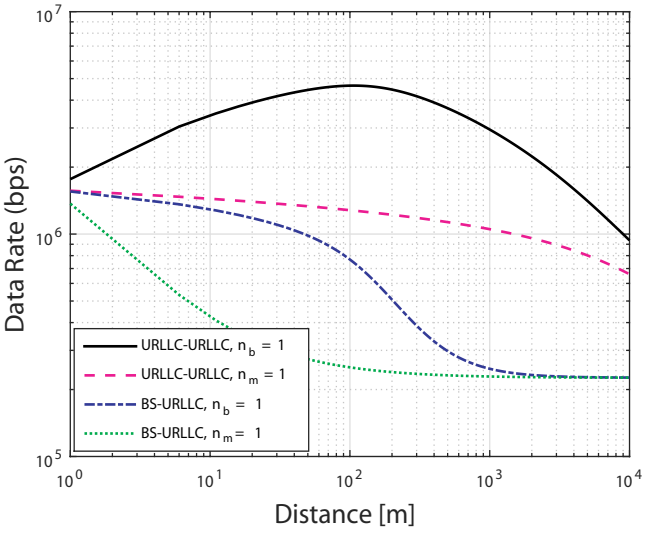

FIGURE 13. Data Rate versus distance for URLLC communications, using optimal transmission power (unconstrained optimization) in THz band.

is 36.55 dBm for mMTC, which is 2.7% lower than optimum power 37.57 dBm required for best case URLLC ($n_b = 1$) and 15.9% lower than optimal power 43.45 dBm required for worst case URLLC ($n_m = 1$). For B2M, at distance of 500 m, optimum power required for mMTC is 57.23 dBm, 2.7% lower than that required for best case URLLC ($n_b = 1$) at 58.82 dBm and 27.89% lower than worst case URLLC ($n_m = 1$) at 79.36 dBm.

Figure 12 shows the data rate vs distance for M2M and B2M mMTC, showing how the data rate decreases with distance between the communicating devices. Figure 13 shows the reducing trend of data rate with distance for each of the URLLC link (note that the initial increase for the M2M URLLC link is due to the decreasing effects on its interference, which enhanced the data rate performance till a certain distance). For M2M, at distance of 100 m the data rate is 5.870×10^6 bps for mMTC, which is 1.3 times higher than data rate, 4.649×10^6 bps, for best case URLLC ($n_b = 1$) and 4.6 times higher than data rate, 1.284×10^6 bps, for worst case URLLC ($n_m = 1$). For B2M, at distance of 500 m, data rate for mMTC is 3.15×10^5 bps, 5.56% higher than that of best case URLLC at 2.975×10^5 bps and 26% higher than worst case URLLC at 2.317×10^5 bps.

Figure 14 shows the plot of energy efficiency versus distance for M2M and B2M mMTC links, while the corresponding curves for URLLC links are shown in Fig. 15. For M2M, at distance of 100 m the energy efficiency is 5.616×10^4 bps/W for mMTC, which is 21.69% higher than corresponding energy efficiency of 4.398×10^4 bps/W for best case URLLC ($n_b = 1$). For B2M, at distance of 500 m, energy efficiency for mMTC is 501.3 bps/W, 1.5 times higher than that achieved for best case URLLC at 345.0 bps/W.

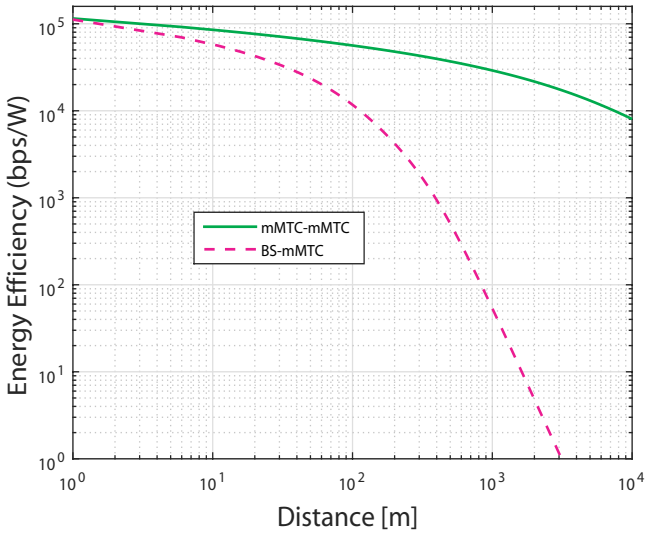

FIGURE 14. Energy efficiency versus distance for mMTC communication with optimal transmission power (unconstrained optimization) in THz band.

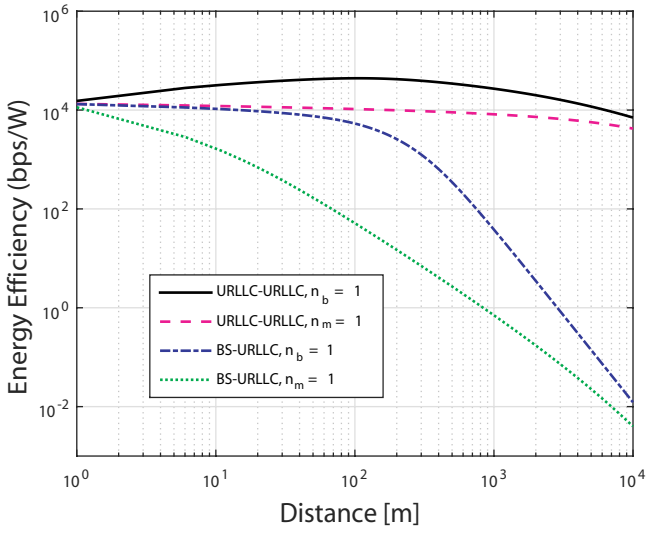

FIGURE 15. Energy efficiency versus distance for URLLC communication with optimal transmission power (unconstrained optimization) in THz band.

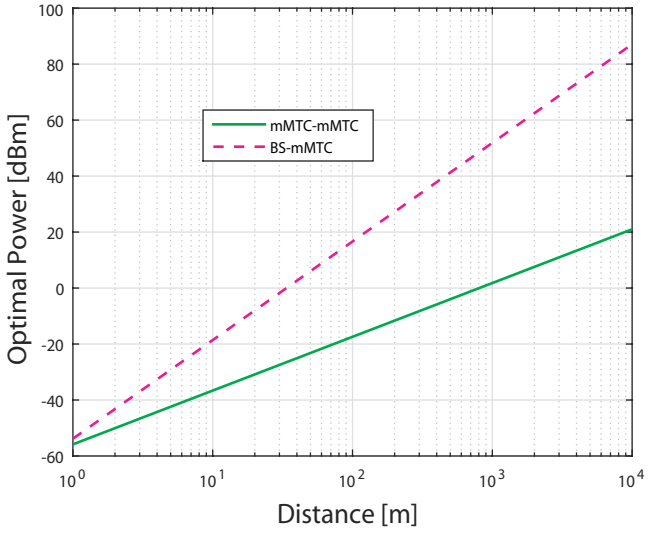

FIGURE 16. Optimal transmission power required versus distance for mMTC communication links (constrained optimization) in THz band.

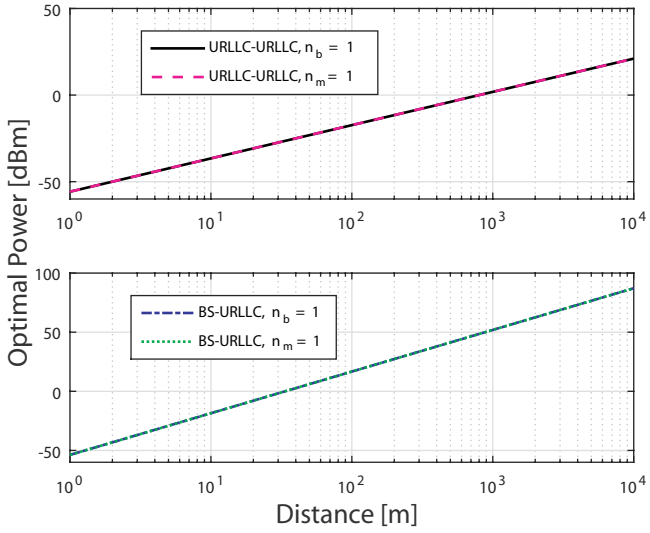

FIGURE 17. Optimal transmission power required versus distance for URLLC communication links (constrained optimization) in THz band.

C. SIMULATIONS AFTER CONSTRAINED OPTIMIZATION

The plots in Figs. 16-19, for constrained optimization, have been simulated using the equation (19), where $R_{th} = 10^5$, and then substituting into equations (11), (12) and (14) for data rate and energy efficiency.

The plots in Figs. 16 and 17, show the trends of optimal transmission power against the distance. With increasing distance between the devices, the path loss and hence the required transmission power increases. At a distance of 100 m the optimal power required is -17.34 dBm for M2M mMTC, lower than optimal power -17.28 dBm required for M2M URLLC. As for B2M, considering the point $d = 500$ m, the optimum power necessary for mMTC is 41.29 dBm, very close to that needed for URLLC at 41.35 dBm.

In Figs. 18 and 19 the plot of energy efficiency versus distance for mMTC and URLLC communication links. Regarding the M2M links, comparing at the distance of 100 m, the energy efficiency obtained is 1000 bps/W for mMTC, the same as 1000 bps/W obtained for M2M URLLC. As for B2M, considering distance of 500 m, the energy efficiency for mMTC is 410.7 bps/W, 8.06% times than that of URLLC at 377.6 bps/W. For this optimization technique, the data rates of mMTC and URLLC links, are all constant (i.e., 10^5) across the entire range of distance. This is because, transmission power increases with an increase in distance, which in turn improves the path loss. Therefore, the channel quality also improves.

V. CONCLUSION

To conclude, in this paper, an application of NOMA for MTC systems in the lower THz band was shown. A system model was presented and equations for the data rate, energy efficiency and optimal transmission power for its different communication links were provided. The performance of

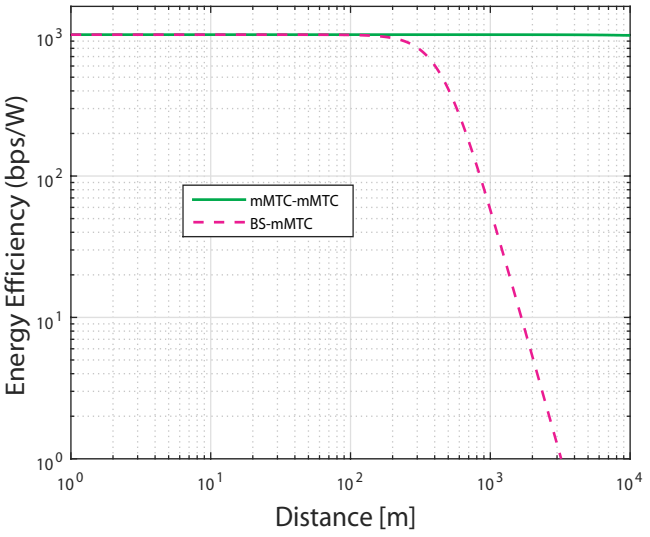

FIGURE 18. Energy efficiency versus distance for mMTC communication with optimal transmission power (constrained optimization) in THz band.

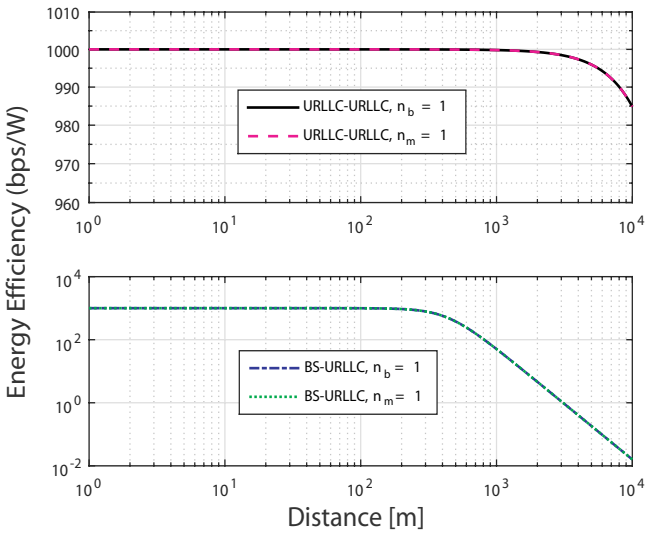

FIGURE 19. Energy efficiency versus distance for URLLC communication with optimal transmission power (constrained optimization) in THz band.

TABLE 3. Comparison between energy efficiency after unconstrained and constrained optimization.

Distance (m)	Communication link	Optimization I: Energy efficiency (no constraints) (bps/W)	Optimization II: Energy efficiency (with constraints) (bps/W)	Performance improvement / drop compared
100	mMTC-mMTC	5.616×10^4	1000	Optimization I > Optimization II (98.22% Drop)
100	URLLC-URLLC ($n_b = 1$)	4.398×10^4	1000	Optimization I > Optimization II (97.73% Drop)
100	URLLC-URLLC ($n_m = 1$)	1.048×10^4	1000	Optimization I > Optimization II (90.46% Drop)
500	BS-mMTC	501.3	410.7	Optimization I > Optimization II (18.07% Drop)
500	BS-URLLC ($n_b = 1$)	345.0	377.6	Optimization II > Optimization I (8.63% Improvement)
500	BS-URLLC ($n_m = 1$)	2.683	377.6	Optimization II > Optimization I (99.29% Improvement)

the model in terms of data rate, optimal transmission power and energy efficiency was evaluated and the plots from simulations were given. The optimization of the transmission power for maximum energy efficiency was derived via unconstrained and constrained optimization. Based on the trends of the plots and the numerical results as shown in Table 3, the following points are to be noted:

1) Implementing the proposed NOMA based system model in the lower THz band frequencies attains better overall performance with respect to data rate and energy efficiency than in lower frequencies such as the mmWave band.
2) The channel gain characteristics were better for M2M than B2M, so M2M communications attained higher data rate over B2M communications. The higher data rate of M2M led to its higher energy efficiency over B2M.
3) Using unconstrained optimization method, the optimal transmission power that was derived led to higher energy efficiency for all M2M communications at 100 m and for the B2M mMTC communication at 500 m, than the transmission power derived using constrained optimization method. On the other hand, the energy efficiency attained using constrained optimization method, led to a higher energy efficiency for both cases of the B2M URLLC communications at 500 m.
4) Thus, the best performance with regard to energy efficiency of the system model presented in this paper can be achieved by utilizing an integral use of two different techniques for the two types of communication links: unconstrained optimization for M2M communications and constrained optimization for B2M communica-

tions.

Based on the results and the research done for this study, we observed the potential of the lower THz band to improve the data rate and energy efficiency of MTC systems. Operating in this band, in conjunction with power domain multiplexing of NOMA and subcarrier sharing over OFDMA, can provide accommodation to a much greater number of wireless devices. The optimization techniques have been useful in resolving the question of power allocation for the differently powered devices in NOMA. Because low powered devices too have been optimized for energy efficiency, we believe that our techniques have enabled the best use of communication resources in protecting signal quality. In future works, further enhancements of this paper's model can be made by incorporating other promising techniques such as transmit antenna selection [27] and energy harvesting [28].

.

APPENDIX A PROOF OF OPTIMAL TRANSMISSION POWER VIA UNCONSTRAINED OPTIMIZATION

Energy efficiency as given in equation (14) expanded is of the form:

$$EE = \frac{B \cdot \log_2\left(1+\frac{p_t|h|^2}{N_oB+I}\right)}{P_{idle}+p_t} = \frac{B}{\ln(2)} \cdot \frac{\ln\left(1+\frac{p_t|h|^2}{N_oB+I}\right)}{P_{idle}+p_t}. \quad \text{(A.1)}$$

Now we derive the equation (A.1) with respect to p_t. We get

$$\frac{d(EE)}{dp_t} = \frac{B}{\ln 2} \cdot \frac{\frac{(P_{idle}+p_t)\cdot|h|^2}{(N_oB+I)\cdot(1+\frac{p_t|h|^2}{N_oB+I})} - \ln(1+\frac{p_t|h|^2}{N_oB+I})}{(P_{idle}+p_t)^2}. \quad \text{(A.2)}$$

Equating (A.2) to zero and changing sides leads to the following equation:

$$\frac{(P_{idle}+p_t)\cdot|h|^2}{N_oB+I} = \left(1+\frac{p_t|h|^2}{N_oB+I}\right)\cdot\ln\left(1+\frac{p_t|h|^2}{N_oB+I}\right). \quad \text{(A.3)}$$

Now we consider

$$e^f = 1+\frac{p_t|h|^2}{N_oB+I}, \quad \text{(A.4)}$$

where f is a variable.

Changing sides, variable f can be expressed as:

$$f = \ln\left(1+\frac{p_t|h|^2}{N_oB+I}\right). \quad \text{(A.5)}$$

Plugging in equation (A.5) in equation (A.4), the following are produced:

$$\frac{P_{idle}\cdot|h|^2}{N_oB+I} + e^f - 1 = e^f\cdot\ln(e^f)$$
$$\Rightarrow \frac{P_{idle}\cdot|h|^2}{N_oB+I} - 1 = (f-1)\cdot e^f. \quad \text{(A.6)}$$

Multiplying both sides of by e^{-1}, we get:

$$e^{-1}\cdot\frac{P_{idle}\cdot|h|^2}{N_oB+I} - 1 = (f-1)\cdot e^{f-1}. \quad \text{(A.7)}$$

Using the inverse of Lambert function, the right and hence the left side of the equation (A.7) can be written as:

$$W\left[e^{-1}\cdot\frac{P_{idle}\cdot|h|^2}{N_oB+I} - 1\right] = f-1. \quad \text{(A.8)}$$

Equation (A.5) can be plugged into equation (A.8) to arrive at:

$$f = \ln\left(1+\frac{p_t|h|^2}{N_oB+I}\right) = 1+W\left[e^{-1}\cdot\frac{P_{idle}\cdot|h|^2}{N_oB+I} - 1\right]. \quad \text{(A.9)}$$

Finally, changing side yields the expression for optimal transmission power for maximum energy efficiency.

APPENDIX B PROOF OF OPTIMAL TRANSMISSION POWER VIA CONSTRAINED OPTIMIZATION

Based on equation (18), the Lagrangian expression [29] can be expressed as

$$\mathcal{L}(p_t) = p_t + \lambda_1\cdot(R_{th}-R) + \lambda_2\cdot(p_{th}-p_t), \quad \text{(B.1)}$$

where λ_1 and λ_2 are Lagrangian multipliers corresponding to constraints (18b) and (18c).

The Lagrangian is differentiated with respect to p_t, λ_1, λ_2 and $|h|^2$ and then equated to zero each time to get the following equations:

$$\frac{d\mathcal{L}}{dp_t} = -\lambda_2 - \frac{B\cdot|h|^2\cdot\lambda_1}{(I+N_oB)\cdot\ln(2)\cdot(1+\frac{|h|^2\cdot p_t}{I+N_oB})} + 1 = 0$$
$$\Rightarrow \lambda_2 = 1 - \frac{B\cdot|h|^2\cdot\lambda_1}{(I+N_oB)\cdot\ln(2)\cdot(1+\frac{|h|^2\cdot p_t}{I+N_oB})}. \quad \text{(B.2)}$$

$$\frac{d\mathcal{L}}{d|h|^2} = -\frac{B\cdot p_t\cdot\lambda_1}{(I+N_oB)\cdot\ln(2)\cdot(1+\frac{|h|^2\cdot p_t}{(I+N_oB)})} = 0$$
$$\Rightarrow \lambda_1 = 0. \quad \text{(B.3)}$$

$$\frac{d\mathcal{L}}{d\lambda_1} = R_{th} - \frac{B\cdot\ln(1+\frac{|h|^2\cdot p_t}{I+N_oB})}{\ln(2)} = 0$$
$$\Rightarrow R_{th} = \frac{B\cdot\ln(1+\frac{|h|^2\cdot p_t}{I+N_oB})}{\ln(2)}. \quad \text{(B.4)}$$

$$\frac{d\mathcal{L}}{d\lambda_2} = p_{th} - p_t = 0$$
$$\Rightarrow p_t = p_{th}. \quad \text{(B.5)}$$

From equation (B.4),

$$\ln(2)R_{th} = B \cdot \ln\left(1 + \frac{|h|^2 \cdot p_t}{I + N_o B}\right)$$
$$\Rightarrow \ln\left(1 + \frac{|h|^2 \cdot p_t}{I + N_o B}\right) = \frac{\ln(2)R_{th}}{B}$$
$$\Rightarrow 1 + \frac{|h|^2 \cdot p_t}{I + N_o B} = \exp\left(\frac{\ln(2)R_{th}}{B}\right)$$
$$\Rightarrow p_t = \frac{I + N_o B}{|h|^2}\left[\exp\left(\frac{\ln(2)R_{th}}{B}\right) - 1\right]. \quad \text{(B.6)}$$

Plugging the expression for λ_1 found in equation (B.3) into equation (B.2) evaluates λ_2 to $\lambda_2 = 1$. Finally, plugging in expressions for λ_1 and λ_2 into equation (B.1):

$$\mathcal{L}(p_t) = p_t + 0 \cdot (R_{th} - R) + 1 \cdot (p_{th} - p_t). \quad \text{(B.7)}$$

And thus, the Lagrangian expression is

$$\mathcal{L}(p_t) = p_{th} = p_t. \quad \text{(B.8)}$$

REFERENCES

[1] K. Schwab, The Fourth Industrial Revolution, Crown Publishing Group, New York, 2017.

[2] T. S. Rappaport, Y. Xing, O. Kanhere, S. Ju, A. Madanayake, S. Mandal, A. Alkhateeb, G. C. Trichopoulos, "Wireless communications and applications above 100 GHz: Opportunities and challenges for 6G and beyond," *IEEE Access*, vol. 7, pp. 78729-78757, 2019.

[3] H. Elayan, O. Amin, R. M. Shubair, M-S. Alouini, "Terahertz communication: The opportunities of wireless technology beyond 5G," in *Proc. International Conference on Advanced Communication Technologies and Networking (CommNet)*, 2018.

[4] V. Petrov, A. Pyattaev, D. Moltchanov, and Y. Koucheryavy, "Terahertz band communications: Applications, research challenges, and standardization activities," in *Proc. 8th International Congress on Ultra Modern Telecommunications and Control Systems and Workshops (ICUMT)*, Dec. 2016.

[5] Y. Saito, Y. Kishiyama, A. Benjebbour, T. Nakamura, A. Li, and K. Higuchi, "Non-orthogonal multiple access (NOMA) for cellular future radio access," in *Proc. of the IEEE 77th Vehicular Technology Conference (VTC'13)*, pp. 1-5, Dresden, Germany, June 2013.

[6] M. Vaezi and H. V. Poor, "NOMA: An information-theoretic perspective," in *Multiple Access Techniques for 5G Wireless Networks and Beyond*, Springer International Publishing, pp. 167-193, Aug. 2018.

[7] L. Feltrin, G. Tsoukaneri, M. Condoluci, C. Buratti, T. Mahmoodi, M. Dohler, and R. Verdone, "Narrowband IoT: A survey on downlink and uplink perspectives," *IEEE Wireless Communications*, vol. 26, no. 1, pp. 78-86, Feb. 2019.

[8] A. E. Mostafa, Y. Zhou, and V. W. Wong, "Connectivity maximization for narrowband IoT systems with NOMA," in *Proc. IEEE International Conference on Communications (ICC)*, 2017.

[9] H. Ji, S. Park, J. Yeo, Y. Kim, J. Lee, and B. Shim, "Ultra-reliable and low-latency communications in 5G downlink: Physical layer aspects," *IEEE Wireless Communications*, vol. 25, no. 3, pp. 124-130, 2018.

[10] Z. Chen, Z. Ding, P. Xu and X. Dai, "Optimal precoding for a QoS optimization problem in two-user MISO-NOMA downlink," *IEEE Communications Letters*, vol. 20, no. 6, pp. 1263-1266, June 2016.

[11] Z. Ding, X. Lei, G. K. Karagiannidis, R. Schober, J. Yuan, and V. K. Bhargava, "A survey on non-orthogonal multiple access for 5G networks: Research challenges and future trends," *IEEE Journal on Selected Areas in Communications*, vol. 35, no. 10, pp. 2181-2195, Jul. 2017.

[12] F. Fang, H. Zhang, J. Cheng, and V. C. Leung, "Energy efficiency of resource scheduling for non-orthogonal multiple access (NOMA) wireless network," in *Proc. IEEE International Conference on Communications (ICC)*, Jul. 2016.

[13] H. Zhang, F. Fang, J. Cheng, K. Long, W. Wang, and V. C. M. Leung, "Energy-efficient resource allocation in NOMA heterogeneous networks," *IEEE Wireless Communications*, vol. 25, no. 2, pp. 48-53, Apr. 2018.

[14] H. Zhang, B. Wang, C. Jiang, K. Long, A. Nallanathan, V. C. M. Leung, and H. V. Poor, "Energy efficient dynamic resource optimization in NOMA system," *IEEE Transactions on Wireless Communications*, vol. 17, no. 9, pp. 5671-5683, Jun. 2018.

[15] P. Wu, J. Zeng, X. Su, H. Gao and T. Lv, "On energy efficiency optimization in downlink MIMO-NOMA," in *Proc. IEEE International Conference on Communications (ICC)*, pp. 399-404, Jul. 2017.

[16] M. Zeng, A. Yadav, O. A. Dobre, G. I. Tsiropoulos and H. V. Poor, "Capacity comparison between MIMO-NOMA and MIMO-OMA with multiple users in a cluster," *IEEE Journal on Selected Areas in Communications*, vol. 35, no. 10, pp. 2413-2424, Oct. 2017.

[17] M. Zeng, A. Yadav, O. A. Dobre, G. I. Tsiropoulos and H. V. Poor, "On the sum rate of MIMO-NOMA and MIMO-OMA systems," *IEEE Wireless Communications Letters*, vol. 6, no. 4, pp. 534-537, Aug. 2017.

[18] S. M. R. Islam, M. Zeng, O. A. Dobre and K. Kwak, "Resource allocation for downlink NOMA systems: Key techniques and open issues," *IEEE Wireless Communications*, vol. 25, no. 2, pp. 40-47, April 2018.

[19] M. Chen, Y. Miao, Y. Hao and K. Hwang, "Narrow band internet of things," *IEEE Access*, vol. 5, pp. 20557-20577, 2017.

[20] 3GPP, TR 25.814 V7.1.0, Release 7, Technical Specification Group Radio Access Networks Physical layer aspects for evolved Universal Terrestrial Radio Access (UTRA), Sept. 2006.

[21] ITU-R report M.2135, Guidelines for evaluation of radio interface technologies for IMT-Advanced, 2008.

[22] H. Xing and S. Hakola, "The investigation of power control schemes for a device-to-device communication integrated into OFDMA cellular system," in *Proc. 21st Annual IEEE International Symposium on Personal, Indoor and Mobile Radio Communications*, pp. 1775-1780, 2010.

[23] G. Wu, C. Yang, S. Li, and G. Y. Li, "Recent advances in energy-efficient networks and their application in 5G systems," *IEEE Wireless Communication*, vol. 22, no. 2, pp. 145-151, Apr. 2015.

[24] M. R. Mili, L. Musavian, K. A. Hamdi and F. Marvasti, "How to increase energy efficiency in cognitive radio networks," *IEEE Transactions on Communications*, vol. 64, no. 5, pp. 1829-1843, May 2016.

[25] K. Miettinen, Nonlinear Multiobjective Optimization, Springer, 1999.

[26] M. R. Akdeniz, Y. Liu, M. K. Samimi, S. Sun, S. Rangan, T. S. Rappaport and E. Erkip, "Millimeter wave channel modeling and cellular capacity evaluation," *IEEE Journal on Selected Areas in Communications*, vol. 32, no. 6, pp. 1164-1179, June 2014.

[27] S. R. Sabuj and M. Hamamura, "Outage and energy-efficiency analysis of cognitive radio networks: A stochastic approach to transmit antenna selection," *Pervasive and Mobile Computing*, Elsevier, vol. 42, pp. 444-469, 2017.

[28] S. R. Sabuj and M. Hamamura, "Two-slope path-loss design of energy harvesting in random cognitive radio networks," *Computer Networks*, Elsevier, vol. 142, pp. 128-141, 2018.

[29] S. Boyd and L. Vandenberghe, Convex Optimization. Cambridge, UK: Cambridge University Press, 2004.

A M MUSA SHAKIB KHAN is currently a final semester student of Electrical and Electronic Engineering (EEE) at Brac University, Dhaka, Bangladesh. His concentration within EEE is in Communications and Computers.

His research interest lies in technologies that facilitate 5G wireless communication (and beyond) such as multiple-access techniques, multiple input multiple output systems and means of optimizing communication for maximum performance and efficiency. He also studies software and hardware architectures of embedded systems, such as those constituting the Internet of things or having biomedical applications.

Mr. Khan has been awarded merit and performance scholarships at Brac University and was also a recipient of scholarship at McGill University, where he had previously studied for a number of semesters.

SAIFUR RAHMAN SABUJ (M'16) was born in Bangladesh in 1985. He received a B. Sc in Electrical, Electronic and Communication Engineering from Dhaka University, Bangladesh in 2007, an M. Sc Engineering in the Institute of Information and Communication Technology, Bangladesh University of Engineering and Technology, Bangladesh in 2011, and a Ph.D. degree in the Graduate School of Engineering, Kochi University of Technology, Japan in 2017.

From 2008 to 2013, he was a faculty member of Green University of Bangladesh, Metropolitan University, Sylhet and Bangladesh University. He has been in the position of an Assistant Professor in the department of Electrical and Electronic Engineering at Brac University, Bangladesh, since September 2017. He is currently working with Electronics and Control Engineering Department as a Postdoctoral Research Fellow at Hanbat National University, South Korea. His research interests include MIMO-OFDM/NOMA, Cooperative Communication, Cognitive Radio, Internet of things, and Machine-to-machine for wireless communications.

MASANORI HAMAMURA (M'00) received his B.S., M.S. and Ph.D. degrees in electrical engineering from Nagaoka University of Technology, Nagaoka, Japan, in 1993, 1995 and 1998, respectively. From 1998 to 2000, he was a Research Fellow of the Japan Society for the Promotion of Science.

Since 2000, he has been with the Department of Information Systems Engineering at Kochi University of Technology, Kochi, Japan, where he is now a Professor. From 1998 to 1999, he was a visiting researcher at Centre for Telecommunications Research, King's College London, United Kingdom, where he worked on adaptive signal processing for mobile systems. His current research interests are in the areas of signal design, wireless communications and signal processing.

Original Manuscript ID: Access-2019-47015

Original Article Title: "Application of Non-Orthogonal Multiple Access for Machine Type Communication in Terahertz Band"

To: IEEE Access Editor

Re: Response to reviewers

Dear Editor,

Thank you for allowing a resubmission of our manuscript, with an opportunity to address the reviewers' comments.

We are uploading (a) our point-by-point response to the comments (below) (response to reviewers), (b) an updated manuscript with yellow highlighting indicating changes, and (c) a clean updated manuscript without highlights (PDF main document). We would like our resubmitted manuscript to be assigned to the same reviewers as before.

We are grateful to the reviewers for helping us improve the quality of our paper.

Best regards,

A M Musa Shakib Khan

Saifur Rahman Sabuj

Masanori Hamamura

Associate Editor at IEEE Access, Concern # 1:

1) Why do the authors think 0.09-0.1 THz is THz? Usually we treat the 300 GHz band as the THz. Thus, the authors should change the title.

Author response:

While some papers [1] suggested that THz band was defined to be frequencies above 100 GHz (also identified as 0.1 THz), there were others [2] [3] who considered frequencies above 300 GHz to be the THz band. However, based on the comments of the Associate Editor and reviewer # 2, we have decided to avoid confusions and have chosen frequencies above 100 GHz for our simulations. We believe our paper is now more in line with the definition of the THz band to be above 300 GHz and has therefore improved (our new calculations are shown below). We hope that doing so has addressed the reviewers' concerns.

Author action:

We updated the manuscript by replacing the previous spectrum with a higher spectrum of 300 GHz, with cut-offs at 0.39 THz and 0.09 THz. This places the channel much higher than our previous 0.1 THz. Based on these new parameters, we re-derived all equations of path-loss and performed simulations again.

"Calculations for determining the bandwidth of this resource block are considered BW = $f_U - f_L$ = (0.39−0.09) THz = 300 GHz. For a large resource block of bandwidth 20 MHz, LTE physical layer standard uses OFDM to raise 1201 SCs [20]. In this paper the principle of OFDM is used to raise 1201 SC frequencies from each of 400 resource blocks, each SC with a bandwidth of approximately 500 KHz."

While this resulted in different data rate and energy efficiency for the various communication links of our mode, as indicated by the graphs, the trends did not vary and thus the ultimate conclusion of the paper has remained the same. We updated the paper with new values for the figure descriptions (please see the yellow highlighted sections in the highlighted PDF between pages 7 - 12) and in Tables 2 (page 9) and 3 (page 13).

Associate Editor at IEEE Access, Concern # 2:

2) Why do the authors use 80 MHz for the bandwidth of a resource block at THz? The benefit of using so high frequencies is to obtain large bandwidth but it is not shown in this paper.

Author response:

We thank the reviewer for pointing out this concern. Our calculations, even based on the 100 GHz spectrum, should have evaluated to 80 GHz and not 80 MHz as we incorrectly wrote in our submitted paper. We apologize for this error on our part. Having now chosen a higher spectrum of 300 GHz, the bandwidth of each of the 1201 SC frequencies from the 400 resource blocks in THz has now increased to 500 KHz (from our previous 66KHz). This has resulted in an increase in data rate and energy efficiency performance for M2M communications. For B2M however, the increase in path loss at higher frequencies, has resulted in decreased performance. Thus an effort to obtain larger bandwidths by moving up frequencies can result in better performance in short distances but lower performance at longer distances of communication.

Author action:

Taking action in response to the first concern has resulted in adjusting for the second concern as well (the following is from page 2 of our paper, as already shown above):

"Calculations for determining the bandwidth of this resource block are considered BW = $f_U - f_L$ = (0.39−0.09) THz = 300 GHz. For a large resource block of bandwidth 20 MHz, LTE physical layer standard uses OFDM to raise 1201 SCs [20]. In this paper the principle of OFDM is used to raise 1201 SC frequencies from each of 400 resource blocks, each SC with a bandwidth of approximately 500 KHz. "

The figure descriptions (please see the yellow highlighted sections in the highlighted PDF between pages 7 - 12) and Tables 2 (page 9) and 3 (page 13) reflect the change resulting from using higher bandwidths.

Reviewer#1, Concerns:

Author response:

We thank Reviewer 1 for his positive review and comments on our paper. Reviewer 1 has presented no concerns, but did suggest minor edits. We have made some changes based on the reviews of the Associate Editor and Reviewer 2. We hope these changes have improved the paper.

Author action:

Not applicable based on Reviewer 1's review.

Reviewer#2, Concern # 1:

Kindly, Provide the peculiarity of the THz band channel and the challenges you have faced to implement it?

Author response:

We did attempt to highlight some of the challenges posed by working in the THz band. For example, on page 2 we had the following mentioned: *"One of the major drawbacks of the technology, however, is that operating in frequencies above 1 THz results in considerable propagation losses, thus severely limiting the range of communication. Considering how operating in the lower THz bands has enabled covering a reasonable range of distance [4], this paper has carried out analysis in the lower part of this spectrum."* This drawback makes the THz band a peculiar one to work with, as it involves drawing a compromise between bandwidth and path loss. This in turn results in a compromise between achievable performance in shorter distances versus longer ones. Regardless, we thought it might be important to address the reviewer's concern by expanding on this more explicitly.

Author action:

In order to address the reviewer's concern, we added the following on page 4, under the heading of III) System Model in an attempt to highlight the peculiarity and challenge of operating in the THz band:

Implementing a model in the THz band is challenging because of its peculiarity: even though higher frequencies enable acquiring of greater bandwidth, which could lead to better communication performance, they also lead to significant path loss that diminishes performance. This calls for the careful selection of a spectrum for our model that not only meets the accepted definition of the THz band but also enables an appreciable level of communication performance.

We also pointed out in our conclusion on page 14 how our optimization techniques helped overcome the challenge of communicating with low powered mMTC devices utilizing NOMA in the THz band. Low powered communicating devices may have poor signal quality and hence lower communication performance.

The optimization techniques have been useful in resolving the question of power allocation for the differently powered devices in NOMA. Because low powered devices too have been optimized for energy efficiency, we believe that our techniques have enabled the best use of communication resources in protecting signal quality.

Reviewer#2, Concern # 2:

Furthermore, consider a channel above 0.1 THz, as I know below that it considered an mm-wave channel.

Author response:

As already mentioned under the response to the Associate Editor, while some papers [1] suggested that THz band was defined to be frequencies above 100 GHz (0.1 THz), there were others [2], [3] who considered THz band to be that above 300 GHz (0.3 THz). However, based on the comments of the Associate Editor and reviewer # 2, we have now decided to avoid confusions and have chosen frequencies above 100 GHz for our simulations. We hope that doing so has addressed the reviewers' concerns.

Author action:

We updated the manuscript by replacing the previous spectrum with a higher spectrum of 300 GHz, with cut-offs at 0.39 THz and 0.09 THz. This places the carrier higher than our previously used 0.1 THz, at around 0.2 THz. Based on these new parameters, we re-derived all equations of path-loss and performed simulations again.

"Calculations for determining the bandwidth of this resource block are considered BW = $f_U - f_L$ = (0.39−0.09) THz = 300 GHz. For a large resource block of bandwidth 20 MHz, LTE physical layer standard uses OFDM to raise 1201 SCs [20]. In this paper the principle of OFDM is used to raise 1201 SC frequencies from each of 400 resource blocks, each SC with a bandwidth of approximately 500 KHz."

While this resulted in different data rate and energy efficiency for the various communication links of our mode, as indicated by the graphs, the trends did not vary and thus the ultimate conclusion of the paper has remained the same. We updated the paper with new values for the figure descriptions (please see the yellow highlighted sections in the highlighted PDF between pages 7 - 12) and in Tables 2 (page 9) and 3 (page 13).

Reviewer#2, Concern # 3:

NOMA is a well-developed technique, so, I would prefer to remove the first-ever work in this domain.

Author response:

We thank the reviewer for pointing this out. The reviewer is probably referring to our claim in the contributions given on page 2 of our paper that our work was the first to investigate NOMA in the THz band. While NOMA is indeed a well-developed technique, what we, the authors, wanted to mention (but incorrectly wrote otherwise) was that the technique was *one of the first* to be investigated in the THz band, to the best of our knowledge and according to what reviewer 1 of our previous submission mentioned. To quote the reviewer: *"This paper is one of the first investigating NOMA in THz band, and thus, it is important."* Unfortunately we incorrectly wrote that our work was *the first* in the THz domain, which is not the case. It is however one of the first.

Author action:

We updated the manuscript by correcting the referred sentence on page 2 of our work, under the contributions of our paper:

"This is one of the first investigations of NOMA in the THz band and attempts to enable massive connectivity of devices with enhanced communication performance."

References:

[1] H. Elayan, O. Amin, R. M. Shubair, M-S. Alouini, "Terahertz communication: The opportunities of wireless technology beyond 5G," in *Proc. International Conference on Advanced Communication Technologies and Networking (CommNet)*, 2018.

[2] L. Zhu, Z. Xiao, X. Xia and D. Oliver Wu, "Millimeter-Wave Communications with Non-Orthogonal Multiple Access for B5G/6G," in *IEEE Access*, vol. 7, pp. 116123-116132, 2019.

[3] T. S. Rappaport et al., "Wireless Communications and Applications above 100 GHz: Opportunities and Challenges for 6G and Beyond," in IEEE Access, vol. 7, pp. 78729-78757, 2019.

Note: *References suggested by reviewers should only be added if it is relevant to the article and makes it more complete. Excessive cases of recommending non-relevant articles should be reported to ieeeaccesseic@ieee.org*

Date of publication xxxx 00, 0000, date of current version xxxx 00, 0000.
Digital Object Identifier 10.1109/ACCESS.2017.DOI

Application of Non-Orthogonal Multiple Access for Machine Type Communication in Terahertz Band

A M MUSA SHAKIB KHAN[1], SAIFUR RAHMAN SABUJ[2], (MEMBER, IEEE), AND MASANORI HAMAMURA.[3], (Member, IEEE)
[1]Department of Electrical and Electronic Engineering, Brac University, Bangladesh (e-mail: a.m.musa.shakib.khan@g.bracu.ac.bd)
[2]Department of Electronics and Control Engineering, Hanbat National University, South Korea (e-mail: s.r.sabuj@ieee.org)
[3]Graduate School of Engineering, Kochi University of Technology, Japan (e-mail: hamamura.masanori@kochi-tech.ac.jp)
Corresponding author: Saifur Rahman Sabuj (e-mail: s.r.sabuj@ieee.org).

ABSTRACT There is a compelling need to address the problem of accommodating the rapidly growing number of machine type devices engaging in communication within the scarce radio spectrum, in current and forthcoming generations of wireless networks. The coming decades will also witness various novel applications, demanding wireless communication at very high data rate and energy efficiency, which currently favored technologies and techniques are inadequate to support. Because of these reasons, it seems inevitable that wireless communication will have to be facilitated by the efficient utilization of larger bandwidth at higher frequencies. Non-Orthogonal Multiple Access (NOMA) and shifting to higher frequency ranges such as the lower terahertz band, have been considered as solutions to provide space to the increasing number of communicating devices while meeting performance requirements. In this paper a machine type communication system model, utilizing the promising technique NOMA and operating in the lower terahertz band, is developed and analyzed for its performances of data rate and energy efficiency. The use of NOMA in the terahertz band is justified by referring to previous works on each of these techniques as well as by the results of simulations and comparisons with NOMA implemented in the mmWave band. Thereafter the energy efficiency of the proposed model is maximized by using unconstrained optimization and then constrained (by threshold of data rate) optimization, the latter solving a multi-objective problem by the ϵ-constraint method. The optimal transmission power is also derived for both optimization techniques. Finally, simulation results demonstrate that the best case scenario for energy efficiency can be achieved by utilizing unconstrained optimization for machine-to-machine communications and constrained optimization for base-to-machine communications.

INDEX TERMS Data rate, energy efficiency, machine-to-machine communication, mmWave, non-orthogonal multiple access, optimization technique and terahertz.

I. INTRODUCTION

As an exponentially growing number of devices are participating in the Internet of Things (IoT), its impact on individuals, businesses, economies and societies is going to be massive. With estimations of a trillion sensors and billions of users to be connected to the Internet by the year 2021 [1], wireless data traffic, a crucial facilitator of IoT, is thus expected to increase in several folds by 2021. Furthermore, we are witnessing the advent of applications such as virtual and augmented reality, self driving cars, telesurgery, wireless backhaul, etc. In fact, within the next decade there could be even newer applications not envisioned yet. Almost all of these applications will have stringent requirements of low latency, high data rate, spectral and energy efficiency, at a level greater than even fifth generation (5G) networks can provide [2].

Given such a scenario, there is urgency for suitably accommodating users and sensors within the available yet limited frequency spectrum in order to enable the required level of communication. Various technologies and techniques are being investigated to prevent wireless spectrum saturation, e.g., by shifting to higher frequency ranges to obtain required bandwidths or using more efficient means of utilizing the already available frequencies. In [2], Rappaport et al. explain

that required data rates such as those in the order of 100 Gigabits per second may only be available at frequencies beyond the 100 GHz mark.

The frequency spectrum between 100 GHz and 10 THz is identified as the Terahertz (THz) band. Its feasibility of accommodating the increasing number of wireless communication devices and supporting the new applications, is currently being examined. Along with providing vastly greater bandwidth and data rate support, operating in this band is advantageous in terms of robustness in various unfavorable environments, resisting noise from optical sources, supporting strong communication security, etc. without posing any health concern [3]. One of the major drawbacks of the technology, however, is that operating in frequencies above 1 THz results in considerable propagation losses, thus severely limiting the range of communication. Considering how operating in the lower THz bands has enabled covering a reasonable range of distance [4], this paper has carried out analysis in the lower part of this spectrum.

In order to combat spectral saturation, which is a hindrance to the requirements of massive connectivity, researchers have recently demonstrated their interest in non orthogonal multiple access (NOMA). Multiple access (MA) techniques can be broadly classified into orthogonal multiple access (OMA) and NOMA. Although, OMA has been utilized in the present and earlier generations of networks, currently there is consensus that NOMA is essential, and potentially more effective than OMA for the applications and requirements of 5G networks and beyond. NOMA brings better spectral efficiency and throughput to communicating systems than OMA, by assigning the same frequency to multiple users (hence non-orthogonal) while segregating in the power or code domain, thus enabling massive connectivity through the share of communication resources. Furthermore, it also provides better user fairness, lower latency and compatibility with present and upcoming systems of communication [5]. NOMA is not a fundamentally novel technique: from an information theory perspective, the idea of sharing communication resources non orthogonally was understood previously as well. However, despite its potentials over OMA, NOMA implementation was held back primarily due to the level of signal processing and associated processing power required by receivers. For NOMA receivers to discern and detect their anticipated signals from a superposition of various others which reach them, they need to be complex enough to carry out successive interference cancellation (SIC). However, that level of complexity for receivers was deemed unacceptable in the previous generations. Today, with advances in processing power capabilities, there has been a reconsideration of SIC and hence NOMA within the research fields of both academia and industry [6]. Because the migration to higher frequency spectra within the near future seems inevitable, and NOMA appears to be the ideal MA technique, this paper investigates the use of NOMA in the lower THz band, in order to effectively and efficiently utilize the bandwidth in this domain. This establishes the rationale for investigating the integration of these two technologies.

As well as using NOMA, this paper also makes use of orthogonal frequency division multiplexing (OFDM), a multicarrier modulation technique that forms the basis of MA in 4G and LTE systems. OFDM's working principle is to divide the available bandwidth or resource blocks into a number of narrow band, overlapping but orthogonal subcarriers (SCs). OFDM techniques have been used in IoT networks such as downlink Narrow Band IoT (NB-IoT): a standard presented by 3GPP and designed for massive numbers of machine type communication (MTC) devices over long ranges, low rate and energy efficient links. Using narrow bandwidths, the NB-IoT standard has greater coverage than global positioning system/general packet radio service and is also able to filter out relatively more noise, thus yielding better signal to interference and noise ratio (SINR) [7]. In order to investigate how each of the above mentioned technologies integrate, our system model runs over a narrow band in the THz spectrum, utilizing OFDM as well as power domain NOMA to enable each of the OFDM SCs to be shared by multiple devices, segregated by their transmission power levels. Such a communication system should theoretically support a vast number of devices and higher levels of spectral efficiency, than what could have been supported by OFDM systems alone, which allows each SC to be occupied by only one device per time slot [8].

Machine to machine communication is an integral part of the IoT landscape, where various types of sensors and devices independently communicate among themselves, sharing information and collaborating on projects, without being governed centrally. Information that is gathered by these devices are often passed onto actuators in real time control systems. Therefore, the ability to guarantee high levels of reliability and timing may be critical for many such devices. Based on this criterion, two classes of machine type communication devices (MTCDs) exist: (i) ultra reliable low latency communication (URLLC) devices, characterized also by high communication power requirements and (ii) massive machine type communication (mMTC) devices, characterized by much lower cost, power and moderate latency and reliability requirements. The former class of devices is going to be utilized in applications such as autonomous driving, telesurgery and industry automation while the latter class will be functional as metering, monitoring and sensing devices [9]. This paper presents a system model of a wireless network of MTCDs, evaluated for its performance in the downlink scenario, using the aforementioned techniques of NOMA over OFDM SCs in the lower THz band. Hence, the main contributions of this paper are:

- Establishing a case for utilization of NOMA in the lower THz band.
- Proposing a novel system model where four MTCDs utilize NOMA to share one OFDM SC over a narrow, lower THz band of frequency. This is one of the first investigations of NOMA in the THz band and attempts to enable massive connectivity of devices with enhanced

communication performance.

- Derivation of data rate and energy efficiency for various communication links of the proposed model.
- Maximizing energy efficiency of the proposed model, first via unconstrained optimization and then via constrained optimization by formulating a multi-objective problem and solving it with the ϵ-constraint method.
- Highlighting energy efficiency performance of the MTCDs between themselves, observing its maximization with the optimization techniques used and comparing between the techniques.

The organization of the paper henceforth is as follows. Section II discusses related works to this study, section III presents and explains the system model, along with equations of SINR, channel gain, data rate, energy efficiency and optimization techniques for maximum energy efficiency, section IV consists of the results from numerical simulations and discussions of the plots and finally section V concludes the paper with the best scheme for energy efficiency of proposed model and suggestions for future studies.

II. RELATED WORKS

In this section, some of the major works related to the techniques and schemes are briefly highlighted.

In order to unify the existing knowledge on Terahertz communication research, [4] made a comprehensive overview of the technology, highlighting its potential benefits (such as terabit-per-second capacities of communication, smaller transceivers and improved energy efficiency) and the important research challenges to be addressed (e.g., barriers to designing THz electronics and media access control mechanisms, modelling THz communication channels, coverage and deployment strategies, etc.). Furthermore, use cases of the technology and design and performance trade-offs were also discussed. In a more recent literature [3], another review of THz technology was made. The authors cited newer research performed to develop THz channel models, mentioning how one particular study was the first to present single sweep THz measurements which could help in the design of THz transceiver electronics. The paper also mentioned some more use cases of THz technology such as hybrid THz-optical wireless links using THz to assist unmanned air vehicles communication in data centers, heterogeneous mobile networks and 3D beamforming.

With regards to NOMA, its power domain version was put forward as a technology for Future Radio Access (FRA) in [5], along with Successive Interference Cancellation (SIC) for decoding, and shown to exhibit improved capacity and cell-edge throughput performance, without frequency selective channel quality indicator being necessarily available at the base station (BS). In [10], NOMA in a multiple input single output (MIMO) broadcast scenario, with the use of Lagrange method and Newton's iterative algorithms to derive minimum transmission powers (also for certain special cases) and optimum precoding vectors, was found to have competitive performance when compared with performance using the optimal strategy of dirty paper coding. The study presented in [11], summarized NOMA as a concept, differentiated between its types and developments such as single carrier, multi-carrier, MIMO-NOMA, cooperative NOMA, millimeter-wave NOMA, issues with practical implementation and major challenges as of the time of the research.

Due to the requirements of better energy efficiency levels in the wireless communication domain, different algorithms have been used to investigate the performance of various system models of NOMA. In [12], the research in energy efficient resource allocation problem for NOMA was done for the first time. Using simulations, the authors demonstrated the superior energy efficiency and capacity of downlink NOMA over OFDMA systems using their suggested algorithms, which incorporated schemes for assigning subchannels and allocating power between users. Further work on solving NOMA user scheduling and power allocation problems have been done in [13], this time in the context of post-LTE heterogeneous networks by taking into account different levels of channel state information (CSI). Following the application of convex optimization on these areas, the researchers produced schemes to improve NOMA performance, made comparisons with techniques existing till then and concluded that energy efficiency performance of NOMA systems could be improved with effective user scheduling and power allocation schemes. In [14], some of the authors of [12] furthered their previous work by regarding energy efficiency, power availability, quality-of-service, etc., in downlink NOMA. They analyzed their system model for its subchannel and power assignments, using algorithms (founded on matching theory) and Lyapunov optimization with constraints, respectively. In another paper [15], to maximize energy efficiency in a downlink MIMO-NOMA scenario, the authors attempted to optimize user scheduling by applying methods based on signal space alignment (SSA) to reduce complexity and signaling overhead together with aiming to develop an energy efficient power allocation scheme based on sequential convex approximation (SCA).

A number of recent literature demonstrated the excellence of MIMO-NOMA over MIMO-OMA. For example, MIMO-NOMA was shown to have better sum channel capacity, ergodic sum capacity and user fairness than MIMO-OMA in [16], [17]. In [18], the authors provide a divide-and-next-largest-difference-based user pairing algorithm for downlink MIMO-NOMA to ascertain fairness in terms of sum rate gain and then makes a comparison between MIMO-NOMA and MIMO-OMA, to again find the superiority of the former over the latter in terms of outage probability and effective sum rate.

Regarding NB-IoT, the study [19] provided a detailed review of the technology starting from its development history, standardization, its functionality, innovations on the technology, its performances when compared with other LPWAN technologies and applications of NB-IoT. Authors concluded by pointing out the security issues of NB-IoT which need to be attended. An interesting and recent literature [8], pre-

TABLE 1. Related schemes and techniques in NOMA

Reference	Summaries of papers utilizing NOMA	Optimization Technique/Algorithm utilized
[10]	QoS optimization by minimizing transmission power and by deriving optimal precoding vectors.	Lagrange dual problem and Newton's iterative method respectively.
[12]	Optimizing energy efficiency in downlink context through formulation of subchannel and power allocation problem.	Difference of convex programming.
[13]	User scheduling and power allocation in 5G heterogeneous networks considering CSI to improve energy efficiency.	Convex optimization.
[14]	Subchannel resource assignment and power allocation problem, considering energy efficiency, power availability, QoS requirements, etc.	Lyapunov optimization to divide problem into linear and Lagrangian subproblems.
[15]	User scheduling and power allocation of a MIMO-NOMA system are optimized to improve energy efficiency.	SSA method to enhance user scheduling (considering maximum collinearity between users) and SCA method, devolving into convex optimization, to form efficient power allocation scheme.
[16], [17]	Superiority of MIMO-NOMA over MIMO-OMA in terms of sum channel capacity, ergodic sum capacity and user fairness.	Optimized user admission scheme for sum rate and number of users based on SINR threshold.
[18]	Control sum rate gain between NOMA clusters and ensure fairness; show MIMO-NOMA has better outage probability and effective sum rate than MIMO-OMA.	D-NLUPA (divide and next largest difference based user pairing algorithm).
This paper	Downlink scenario, in lower THz, optimized for energy efficiency by deriving optimal transmission power, via unconstrained and constrained techniques.	Formulating single-objective problem via unconstrained optimization and multi-objective problem via constrained optimization then using ϵ-constraint method to simplify into single-optimization problem and solved using Lagrangian function.

sented a power domain NOMA mechanism for MTC in NB-IoT networks. With the aid of such strategy, along with providing algorithms to solve a combined subcarrier and transmission power assignment problem, the authors were able to maximize the total machine type communicating devices that the network could support. Our paper drew inspiration from the ideas presented by the aforementioned work.

III. SYSTEM MODEL

Consider a landscape with a BS and several MTCDs, where machine-to-machine communication (between two MTCDs) and base-to-machine communication (downlink, from BS to MTCD) is shown in Fig. 1. These MTCD (mMTC and uRLLC) communications are designed to occur over a wireless network operating within a band in the lower THz spectrum which is in turn divided into numerous resource blocks. Implementing a model in the THz band is challenging because of its peculiarity: even though higher frequencies enable acquiring of greater bandwidth, which could lead to better communication performance, they also lead to significant path loss that diminishes performance. This calls for the careful selection of a spectrum for our model that not only meets the accepted definition of the THz band but also enables an appreciable level of communication performance. Hence, calculations for determining the bandwidth of this resource block are considered $BW = f_U - f_L = (0.39 - 0.09)$ THz $= 300$ GHz.

For a large resource block of bandwidth 20 MHz, LTE physical layer standard uses OFDM to raise 1201 SCs [20]. In this paper the principle of OFDM is used to raise 1201 SC frequencies from each of 400 resource blocks, each SC with a bandwidth of approximately 500 KHz. Whereas OFDMA in LTE networks today assigns one SC to only one MTCD for communication [8], in our model, NOMA would act on top of OFDMA and enable each SC to be shared by multiple MTCDs as well as the BS, by multiplexing all these devices in the power domain. Using one same SC, a pair of mMTC devices can communicate between themselves while simultaneously a pair of URLLC devices can also communicate between themselves. Moreover, each of these four devices (MTCDs) can individually receive signals from the BS using that same SC. This can be arranged by allocating the URLLC pair with higher transmission power for communication than the mMTC pair, thus segregating the two types of devices using the same SC in the power domain. It is noted that communication is not enabled between a URLLC device and an mMTC device due to their different orders of latency. Also, in this model, the BS addresses each MTCD of a particular type in different time slots but can transmit to an mMTC and a URLLC at the same time. For the rest of the paper, the communication between MTCDs is going to be denoted as "machine-to-machine (M2M)" and the communication between MTCD and the BS as "base-to-machine (B2M)" .

For convenience of evaluating performance some constraints placed on our model are:

1) It is assumed that for a SC, each of the two URLLC devices is at a uniform distance from each mMTC device and similarly each mMTC device is also uniformly spaced from each URLLC device. Otherwise if they are placed at random distances, the channel gains would be different for every device and each would require its own measure of performance, making generalized comparisons of performances complex.
2) The BS transmits to mMTC devices at the same signal power level that the mMTC devices use to communicate with the BS and/or each other. The same applies for URLLC devices. Thus, the transmission power

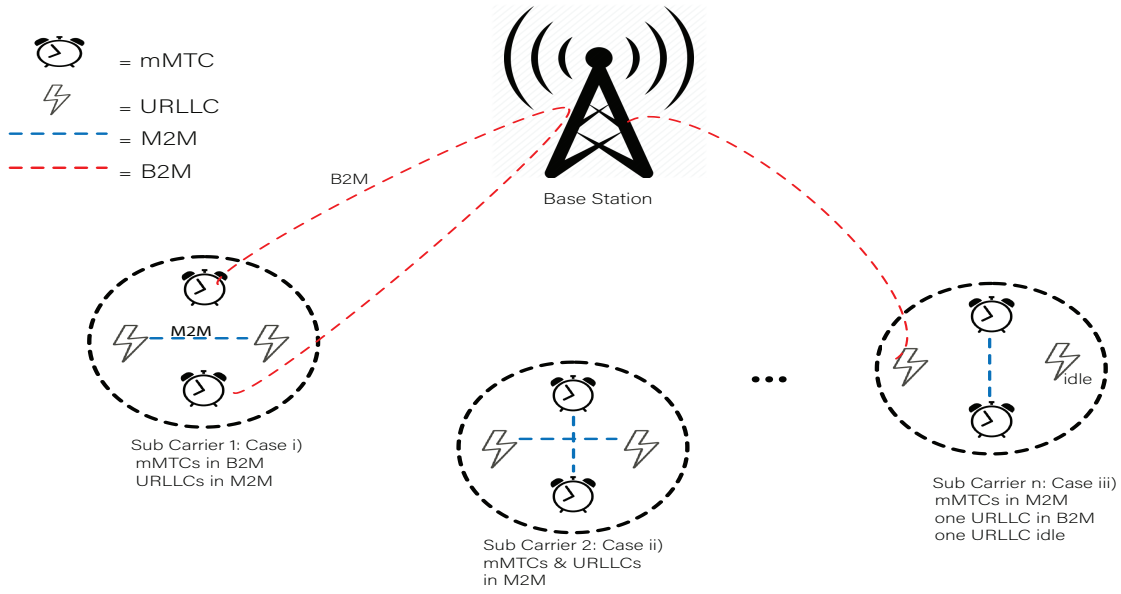

FIGURE 1. Communication links between the MTCDs and the BS.

from the BS to any MTCD and from that MTCD to the BS and the transmission power between MTCDs are all at the same level.

A. SINR WITHIN NOMA SCHEME

With the above constraints in place, we analyze the communication within a particular SC in a downlink context (i.e. in B2M mode, MTCDs are receiving from BS, without transmitting to it). At the receiver of the NOMA communication link, SIC process is performed until the receiver finds its anticipated signal. In the downlink scenario, the BS is transmitting to the MTCDs. In the ideal case, interference may only be possible for devices communicating using the same SC (since they share the same frequencies). Each receiving device needs to perform SIC to decode its own signal from that of others using the same SC. It does so by first detecting signals stronger than its own anticipated signal level, then subtracting them from the total received signal to eventually find its desired signal. Conversely, signals with power that are lower than its own are treated as noise [5].

Consider an mMTC device receiving signals from the BS or another mMTC. mMTC devices operate with signals of lower power levels than that of the lower latency URLLCs. This means that at the mMTC receivers, the arriving higher powered URLLC signals are canceled out by the SIC process and only its anticipated signals are available for decoding. As a result, URLLC devices of the same SC do not cause interference to the communication of the mMTC devices. Based on this, the generic equation of the received SINR of an mMTC device using a particular SC is given by:

$$\gamma_m = \frac{p_m |h_m|^2}{N_o B}, \tag{1}$$

where h_m, p_m, N_o and B denote the channel gain, transmission power, noise power spectral density and the SC bandwidth, respectively. Note that the channel gain changes between the M2M and B2M mode and can be denoted as $h_{m,m}$ and $h_{m,b}$, respectively. Similarly, N_o can be replaced by $N_{o,m}$ or $N_{o,b}$ to represent the different noise levels between the two modes of communication.

For a receiving URLLC device in a SC, lower power signals originating from mMTC devices and, during downlink, from the BS to the mMTC devices pose different levels of interference to the URLLC's anticipated signals. Using SIC, the receiving URLLC device is able to recognize the different power levels of signals, treating these lower power levels (to be denoted by variable "I") as noise to its anticipated level of power signal. Hence, a generalized equation for the received SINR of a URLLC device is given by:

$$\gamma_u = \frac{p_u |h_u|^2}{I + N_o B}, \tag{2}$$

where h_u, p_u, N_o, I and B denote the channel gain, transmission power, the noise power spectral density, the lower power interference and the SC bandwidth, respectively. Again, the channel gain changes between the M2M and B2M mode and can be denoted as $h_{u,u}$ and $h_{u,b}$, respectively. Similarly, N_o can be replaced by $N_{o,u}$ or $N_{o,b}$ between the two modes of communication. The term I is either I_b or I_m. I_b is represented by

$$I = I_b = n_b \cdot p_m \cdot |h_{m,b}|^2, \tag{3}$$

where $n_b = 1$ if BS is transmitting to mMTCs (B2M mode) and $|h_{m,b}|^2$ is the channel gain for the path between the mMTC device and the BS. I_m is represented by

$$I = I_m = n_m \cdot p_m \cdot |h_{m,m}|^2, \tag{4}$$

where the variable $n_m = 1$ is used to show if the mMTC devices are communicating with each other (M2M mode) and $|h_{m,m}|^2$ is the channel gain for the path between the mMTC devices. When $n_b = 1$, n_m must be "0" and vice versa. This is because when mMTC is in B2M mode, it cannot also be in M2M mode (can only communicate with another device or the BS during a particular time frame).

Thus, for the URLLC device in this system model, interference arise either from the I_b or the I_m term, depending on whether the mMTC device sharing the frequency band is in B2M or M2M mode, but not both simultaneously. Note that in the best case scenario, mMTC devices are not communicating at all and hence pose no interference, thereby maximizing SINR for URLLC devices, but we have considered the worst case scenarios here.

B. CHANNEL GAIN FROM PATH LOSS MODEL

Path loss is the attenuation of electromagnetic wave power as it propagates through space from the transmitter to the receiver. For this system model, the channel gain of the various M2M and B2M communication links are derived from the path loss models found in [21], [22]. As pointed out in section I (Introduction), THz band is an upcoming technology with several potential benefits for wireless communications. Hence, considering a carrier in the lower THz band of frequency 0.2 THz (with upper and lower cut-offs of 0.39 THz and 0.09 THz respectively), line of sight (LOS) and non line of sight (NLOS) expressions of path loss for M2M and B2M communications can be given by these expressions:

$$PL_{M2M}^{LOS} = 16.9\log_{10}(d[m]) + 78.8, \quad (5)$$

$$PL_{M2M}^{NLOS} = 40\log_{10}(R[km]) + 208, \quad (6)$$

$$PL_{B2M}^{LOS} = 22\log_{10}(d[m]) + 74, \quad (7)$$

$$PL_{B2M}^{NLOS} = 36.7\log_{10}(d[m]) + 82.6, \quad (8)$$

where d is expressed in m and R is expressed in km. Using the above, the average path loss can be expressed by the following:

$$PL(d) = \alpha \cdot PL_{LOS} + (1-\alpha) \cdot PL_{NLOS}, \quad (9)$$

where α is the probability co-efficient of LOS, PL_{LOS} is the LOS path loss and PL_{NLOS} is the NLOS path loss. For each case above, channel gain $|h|^2$ can be evaluated by the expression:

$$|h|^2 = 10^{-\frac{PL(d)}{10}}, \quad (10)$$

C. EVALUATING PERFORMANCE METRIC

In this section, we analyze the performance metric such as the data rate, energy efficiency and develop optimization techniques for the various M2M and B2M communications of our system model.

1) Data Rate

For an mMTC device, the generic equation for its attainable data rate using the expression for received SINR from equation (1) is given by the following expression:

$$R_m = B \cdot \log_2\left(1 + \frac{p_m |h_m|^2}{N_o B}\right), \quad (11)$$

where the channel gain h_m changes according to the particular mode of the device's communication: M2M or B2M, as explained previously.

Similarly, for a URLLC device, using the SINR expression from equation (2), the following expression gives its attainable data rate:

$$R_u = B \cdot \log_2\left(1 + \frac{p_u |h_u|^2}{I + N_o B}\right), \quad (12)$$

where the channel gain h_u changes according to the particular mode of the device's communication: M2M or B2M.

As explained in equations (3) and (4), the term "I" in the above equation can either be $I = I_b$ or $I = I_m$ depending on whether the mMTC device sharing the frequency band is in M2M or B2M mode.

At this point, it may be useful to produce a generic equation for the data rate of an MTCD device (mMTC or URLLC) for the purpose of evaluating the performance of the system model using some other metrics. This is possible because equations (11) and (12) have similar variables. Thus, the data rate of an MTCD can be expressed as:

$$R = B \cdot \log_2\left(1 + \frac{p_t |h|^2}{I + N_o B}\right), \quad (13)$$

where p_t is the transmission power of the MTCD, $|h|$ being the respective channel gain of the communication link and I being the interference if any (to be present only for URLLC receivers).

2) Energy Efficiency

Energy efficiency is defined as a measure of the number of bits transmitted per joule of consumed energy [23]. In this paper we find this metric by taking the ratio of the data rate to the total power consumption of transmitting devices (i.e. BS or MTCD).

$$EE = \frac{\mathbb{E}[R]}{P_{idle} + \mathbb{E}[p_t]}, \quad (14)$$

where $\mathbb{E}[\cdot]$ denotes the expectation operator, $\mathbb{E}[R]$ is expected value of the data rate from equations (11) and (12), P_{idle} the constant value of power consumed by the transmitting device's circuit and $\mathbb{E}[p_t]$ is expected transmission power.

3) Optimization I: Maximizing Energy Efficiency via Unconstrained Optimization

In this subsection, we attempt to derive the maximum energy efficiency that can be achieved, with respect to transmitting device's power (p_t), without immediately considering any

constraints, and thus not taking into account effect on other performance metrics such as data rate.

The maximum energy efficiency for M2M or B2M communications using equation (13) is represented by:

$$\max_{p_t>0} \frac{\mathbb{E}[R]}{P_{idle}+\mathbb{E}[p_t]}. \tag{15}$$

Taking the derivative of the above equation with respect to p_t, using the generic expression for the data rate of an MTCD from equation (13), the optimal transmission power for which we can attain maximum energy efficiency for M2M or B2M communications is:

$$p_t^{WOC} = \frac{I+N_oB}{|h|^2}\left(e^{1+W\left[e^{-1}\cdot\left(\frac{P_{idle}\cdot|h|^2}{I+N_oB}-1\right)\right]}-1\right), \tag{16}$$

where $W(\cdot)$ is Lambert function.

Proof: The derivation for the above is provided in Appendix A.

4) Optimization II: Maximizing Energy Efficiency via Constrained Optimization

This subsection derives the mathematical expressions for the maximum energy efficiency of our model, this time placing certain constraints on the data rate and binding it to a threshold. This technique may be useful for scenarios where the energy efficiency is required to be maximized without affecting the date rate performance.

In order to improve the energy efficiency performance, as given by equation (14), a multi-optimization problem (MOP) can be created which maximizes the numerator of the ratio (i.e. expected value of the data rate) while minimizing the denominator, i.e, the expected value of transmission power during operation, as shown below:

$$\min_{p_t} \quad \mathbb{E}[p_t] \tag{17a}$$
$$\max_{p_t} \quad \mathbb{E}[R] \tag{17b}$$
$$\text{s.t.} \quad p_t \geq p_{th}. \tag{17c}$$

Using the ϵ-constraint method [24], [25], the MOP problem above can be reduced to a single optimization problem (SOP) by minimizing one parameter while binding the others by allowable thresholds. The following conditions show the SOP problem at hand:

$$\min_{p_t} \quad \mathbb{E}[p_t] \tag{18a}$$
$$\text{s.t.} \quad \mathbb{E}[R] \geq R_{th} \tag{18b}$$
$$\text{s.t.} \quad p_t \geq p_{th}. \tag{18c}$$

Thus, the SOP problem above seeks to minimize the transmission power while binding the data rate to a threshold R_{th} and the transmission power above the threshold p_{th}. Using the Lagrangian method in equations (18a)-(18c), optimal transmission power can be expressed as

$$p_t^{WC} = \frac{I+N_oB}{|h|^2}\left[\exp\left(\frac{\ln(2)R_{th}}{B}\right)-1\right]. \tag{19}$$

Proof: The derivation for the above is provided in Appendix B.

IV. RESULTS AND DISCUSSION

Using the equations for the data rate, energy efficiency and required optimum power of the communication links that are considered in the system model, we have carried out a number of simulations to analyze performance in this section. For the numerical evaluation of above equations, we use the following parameters: $B = 500$ KHz, $N_o = -174$ dBm, $P_{idle} = 100$ W, $\alpha = 0.9$ for M2M and $\alpha = 0.1$ for B2M.

A. SIMULATIONS WITHOUT OPTIMIZATION

The plots in Figs. 2-9 have been performed using equations (11), (12) and (14). In this subsection, the distance between mMTC and mMTC, URLLC and URLLC, BS and mMTC, and BS and URLLC are considered as 100 m, 200 m, 300 m and 400 m, respectively.

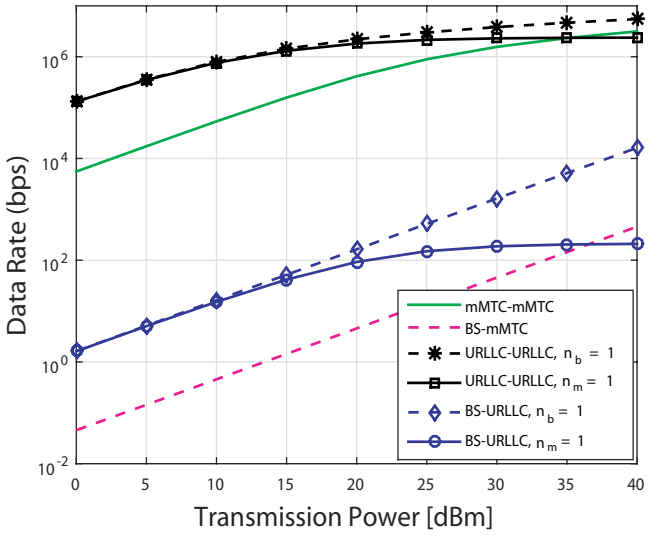

FIGURE 2. Data rate of all communication links versus transmission power in THz band.

Figure 2 shows the simulated plot of data rate versus transmission power of all the communication links discussed in this paper. Higher data rate arises for M2M communication links over B2M links, due to the relatively shorter distance in between the MTCDs in M2M mode than the larger distance between the BS and MTCDs in B2M mode. On the other hand, having greater power allocation than mMTC devices, URLLC communications achieve higher data rates. The legend shows the two cases of URLLC-URLLC links, $n_b = 1$ and $n_m = 1$. In case $n_b = 1$, URLLC-URLLC links attain higher data rate when receiving interference from the BS transmitting to mMTCs, than in case $n_m = 1$, where interference arises due to the mMTCs communicating in M2M mode. The explanation for this is that in case $n_m = 1$, the URLLC devices are nearer to the interfering mMTC transmission, while in case $n_b = 1$, the URLLC devices are farther from the interfering BS transmission. Due to fading

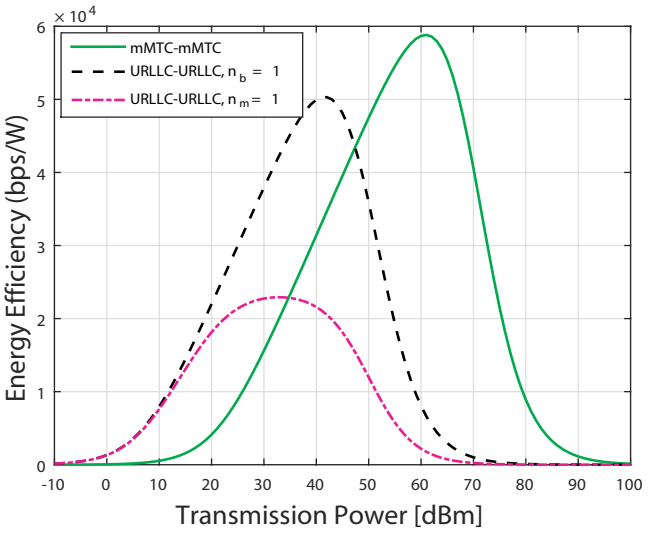

FIGURE 3. Energy efficiency of M2M communication links versus transmission power in THz band.

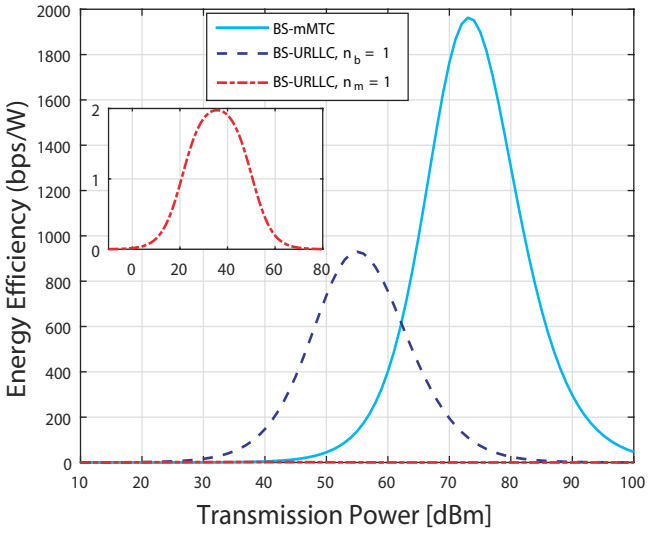

FIGURE 4. Energy efficiency of B2M communication links versus transmission power in THz band.

over longer distances, the BS-mMTC transmission thus has lower impact of interference on URLLC. This phenomenon will also be applicable for the other simulation plots in this paper. In Fig. 2, at $p_t = 25$ dBm, the data rate for the best case URLLC-URLLC ($n_b = 1$) link, at 3.00×10^6 bps, is 3.4 times higher than mMTC-mMTC at 8.90×10^5 bps. On the other hand, the best case BS-URLLC ($n_b = 1$) link at 517.1 bps has 36 times higher data rate than that of mMTC at 14.40 bps.

The plot of energy efficiency versus transmission power for M2M communication links is shown in Fig. 3. Although URLLC devices enjoy greater data rate than mMTCs, the transmission power level allocated to them is relatively much greater. As a result, the energy efficiency of mMTC devices is greater. Energy efficiency of URLLC devices for the case of $n_b = 1$ is higher than that of the case $n_m = 1$, because the data rate of the former communication link is higher than the latter. We can characterize the power for which we have peak (maximum) energy efficiency as the optimum power for these communication links with regards to energy efficiency. Thus, according to this plot, energy efficiency for mMTC-mMTC at the optimum power of 61 dBm is 5.88×10^4 bps/W, which is 14.3% higher than that of URLLC-URLLC (for case $n_b = 1$) at 5.03×10^4 bps/W for its own optimum power of 42 dBm. It is to be noted however, the required optimum power for mMTC is greater than that of URLLC.

Figure 4 shows the plot of energy efficiency versus transmission power for B2M communication links of the system model. As explained for Fig. 3, BS-mMTC link experiences greater peak energy efficiency due to power allocation for its transmission being much less than that of the BS-URLLC link. The peak energy efficiency of the BS-URLLC link for case $n_m = 1$ is justifiably the lowest, due to the lower data rate of the link (due to highest interference experienced) despite utilizing high levels of transmission power. At the

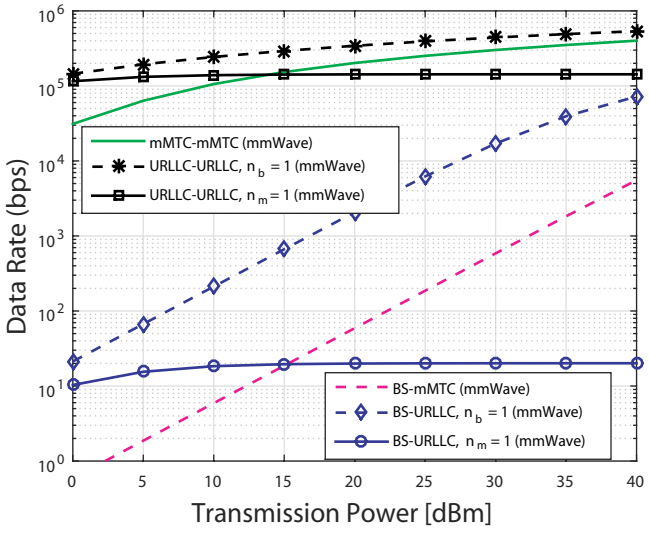

FIGURE 5. Data rate of all communication links versus transmission power in mmWave.

optimum power of 73 dBm, the BS-mMTC link has an energy efficiency of 1963 bps/W. This is 2.1 times higher than energy efficiency of BS-URLLC (case $n_b = 1$), which is 929.8 bps/W at its optimum power of 55 dBm.

An analysis of NOMA in the THz band has not been done in any previous work, as already discussed in section I (Introduction). Therefore in order to evaluate how the system model of our paper based in the lower THz band performs, a comparison with existing techniques such as operating in lower frequencies such as the mmWave band will be useful. While both 28 GHz and 73 GHz provide natural prospects for mmWave deployment [26], our simulations were carried out using the higher of these two frequencies. The path loss models used [21], [22] are as follows: $PL^{M2M}_{mmLOS} = 16.9 \log_{10}(d[m]) + 70.1$, $PL^{M2M}_{mmNLOS} =$

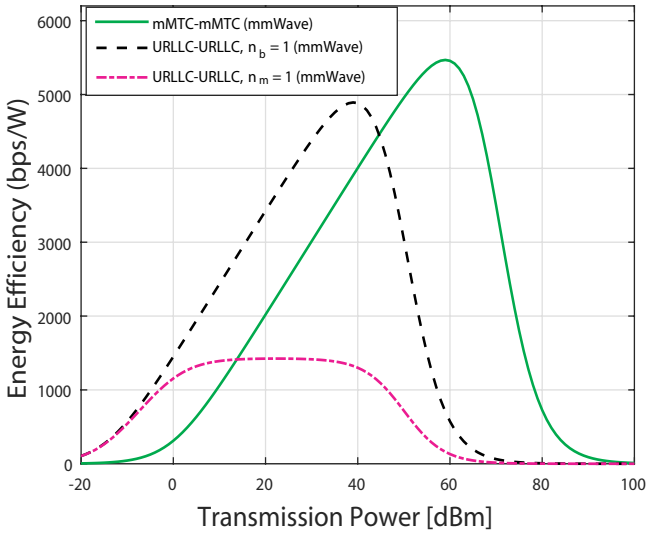

FIGURE 6. Energy efficiency of M2M communication links versus transmission power in mmWave.

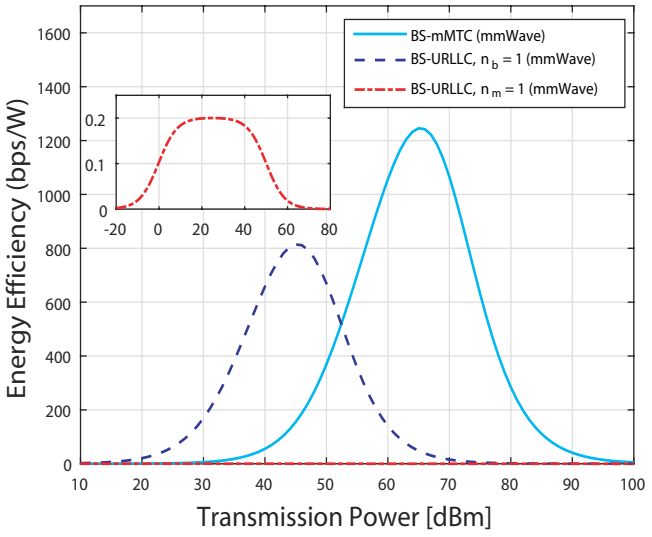

FIGURE 7. Energy efficiency of B2M communication links versus transmission power in mmWave.

TABLE 2. Comparison between the performance of NOMA in lower THz and NOMA in mmWave band.

Communication link	mmWave data rate (bps)	Lower THz data rate (bps)	Comparing data rate - operating in:	mmWave energy efficiency (bps/W)	Lower THz energy efficiency (bps/W)	Comparing energy efficiency - operating in:
mMTC-mMTC	2.52×10^5	8.90×10^5	THz is higher by 3.6 times	5468	5.88×10^4	THz is higher by 11 times
URLLC-URLLC ($n_b = 1$)	3.93×10^5	3.00×10^6	THz is higher by 7.6 times	4893	5.03×10^4	THz is higher by 10 times
BS-mMTC	186.4	14.40	mmWave is higher by 13 times	1245	1963	THz is higher by 1.6 times
BS-URLLC ($n_b = 1$)	6213	517.1	mmWave is higher by 12 times	814.4	929.8	THz is higher by 1.1 times

$40\log_{10}(d[km]) + 194.9$, $PL^{B2M}_{mmLOS} = 22\log_{10}(d[m]) + 65.3$ and $PL^{B2M}_{mmNLOS} = 36.7\log_{10}(d[m]) + 71.2$.

The bandwidth of communication in mmWave is appreciably lower than that in THz band. Theoretically, this should help communication in the THz band to reach higher data rates. At the same time, the path loss in higher frequency bands of operation is also greater, which would counteract signal transmission and hence result in lower rates of communication.

The plot of data rate versus signal transmission power of all communication links of our model based in the mmWave band is shown in Fig. 5. The overall trend or shape of the curves is similar to that of the data rate curves in the lower THz band, for the same reasons as discussed for Fig. 2. Focusing on $p_t = 25$ dBm, as we did for Fig. 2, we find that the data rate for the best case URLLC-URLLC ($n_b = 1$) link is 3.93×10^5 bps, for the mMTC-mMTC link to be 2.52×10^5 bps, for the BS-URLLC ($n_b = 1$) link to be 6213 bps and the BS-mMTC link to be 186.4 bps.

The plot of energy efficiency against transmission power is shown in Figs. 6 and 7. For M2M, the mMTC link has an energy efficiency of 5468 bps/W at optimum transmission power 59 dBm and the URLLC ($n_b = 1$) link is at 4893 bps/W for optimum power of 39 dBm. As for B2M, the mMTC link has energy efficiency of 1245 bps/W at optimum power 65 dBm and URLLC link ($n_b = 1$) has energy efficiency of 814.4 bps/W for optimum power 45 dBm.

Table 2 summarizes and draws a comparison between the performance of NOMA in lower THz and NOMA in mmWave band. According to the table, the THz band outperforms mmWave with regards to data rate for M2M communication, while for B2M communication data rate is higher in the mmWave band than in THz. The explanation for this is that at longer distances of B2M communication, the THz band signals incur significant path loss such that the data rate falls below that of mmWave communication.

In the case of energy efficiency however, THz band outperforms mmWave band for both M2M and B2M communication according to our simulations. We have therefore made the following observations from our analysis in shifting to higher frequencies such as the lower THz band from mmWave band:

- We can expect better performance in terms of energy efficiency for both short and relatively longer range communications.
- We can expect higher data rate for short range M2M

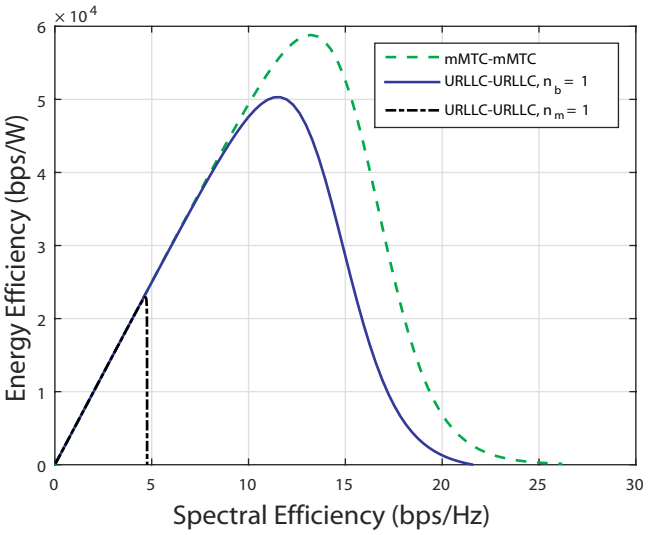

FIGURE 8. Trend of energy efficiency with spectral efficiency of M2M communication links in THz band.

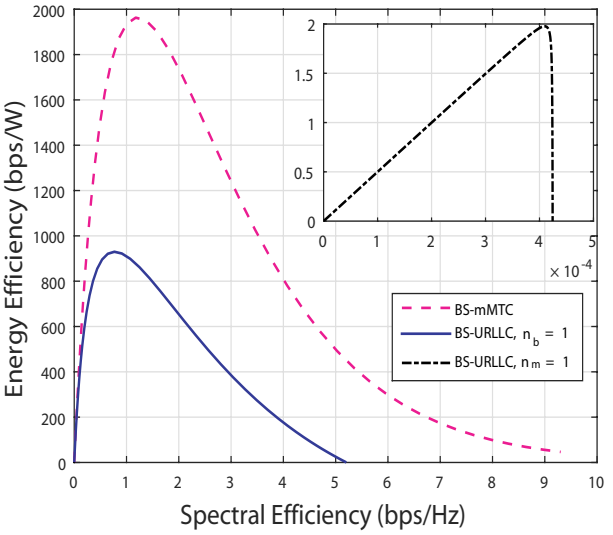

FIGURE 9. Trend of energy efficiency with spectral efficiency of B2M communication links in THz band.

communications while for longer ranged B2M communications, path loss of transmission reduces achievable data rate such that mmWave outperforms THz band operation.

These observations suggest that it may be more beneficial to implement the proposed NOMA based model in the lower THz band than in lower frequencies in order to maximize energy efficiency. Although data rate in mmWave is higher for longer distances than in lower THz, taking the factor of energy efficiency into account makes the lower THz band a better overall choice for our system model.

The plot of energy efficiency versus spectral efficiency for M2M links is shown in Fig. 8, by transmitting power from -10 dBm to 100 dBm. According to the curves, the mMTC link has peak energy efficiency of 5.882×10^4 bps/W at a higher spectral efficiency of 13.24 bps/Hz than the peak energy efficiency with a value of 5.031×10^4 bps/W, of the best case curve for URLLC link ($n_b = 1$) at its spectral efficiency of 11.64 bps/Hz. Comparing, energy efficiency and spectral efficiency of mMTC links are higher than URLLC links by 14.47% and 12.08%, respectively. According to this plot, mMTC seems to outperform URLLC with regards to energy efficiency and spectral efficiency.

Figure 9 shows the plot of energy efficiency versus spectral efficiency for B2M links, by transmitting power from -10 dBm to 100 dBm. For this case, mMTC has peak energy efficiency of 1963 bps/W, which is 2.1 times higher than peak energy efficiency of 929.8 bps/W for URLLC. In addition, spectral efficiency measurement of mMTC link is 34.68% higher (at peak energy efficiency) than spectral efficiency of best case URLLC ($n_b = 1$).

To summarize, in this subsection we observe the data rate, energy efficiency and spectral efficiency performances of our model, with the devices placed at different distances. For M2M, the best case URLLC link ($n_b = 1$) has higher data rate than mMTC communication, while although mMTC communication has potentially better energy efficiency and spectral efficiency performances, to reach these higher levels, mMTC communication requires a much higher transmission power than URLLC. On the other hand, URLLC ($n_b = 1$) communication attains peak energy efficiency using lower transmission power. As for B2M at a longer distance, mMTC outperforms URLLC with regards to data rate and potentially energy and spectral efficiency. However, as with M2M, URLLC ($n_b = 1$) achieves peak energy efficiency at lower transmission power. It seems that at longer distances, the effect of interference becomes very prominent for URLLC links and together with the factor of their high transmission power, result in lower performances in B2M. As for URLLC communication (case $n_m = 1$) witnessed much lower performances in both M2M and B2M scenarios than the other two types of link. Finally, having evaluated the proposed model in both mmWave and lower THz bands, we have determined that, in terms of data rate and energy efficiency, it might be more advantageous to operate in the latter frequencies than in the former.

B. SIMULATIONS AFTER UNCONSTRAINED OPTIMIZATION

The plots in Figs. 10-15, for unconstrained optimization, have been simulated using the equation (16) and then putting equation (16) into equations (11), (12) and (14) for data rate and energy efficiency.

The curves of required optimal transmission power versus the distance for all the communication links are shown in Figs. 10 and 11. As the distance between the communicating devices increase, the power required for transmission justifiably increases (the initial decrease for cases $n_b = 1$ is due to the factor of interference which too reduces with distance). For M2M, at distance of 100 m the optimum power required

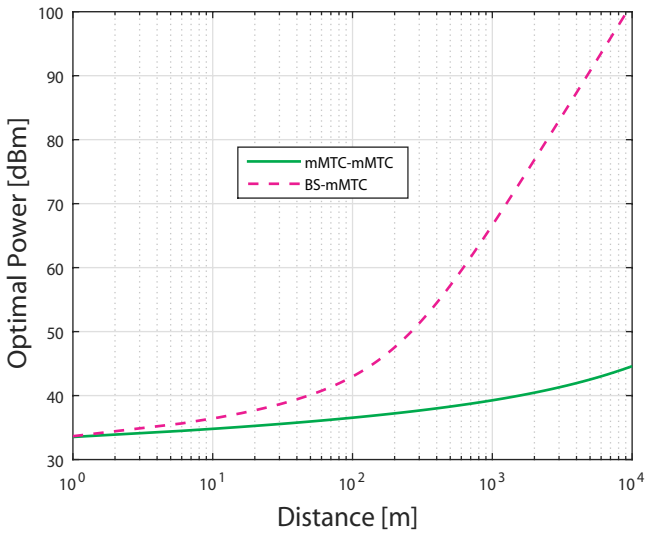

FIGURE 10. Optimal transmission power required versus distance for mMTC communication links (unconstrained optimization) in THz band.

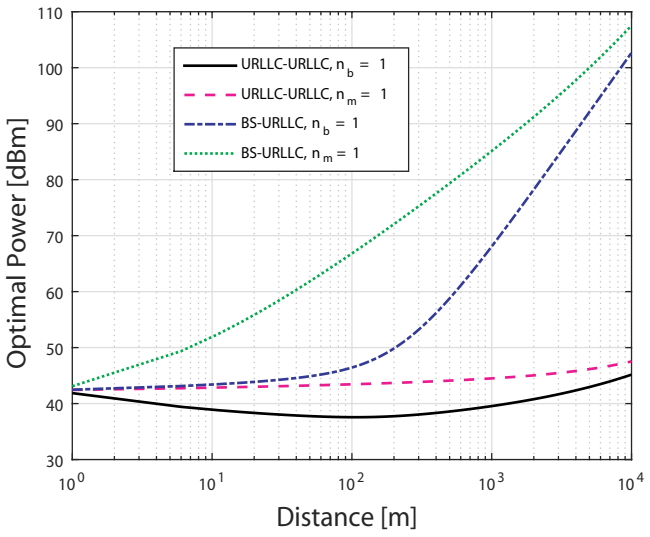

FIGURE 11. Optimal transmission power required versus distance for URLLC communication links (unconstrained optimization) in THz band.

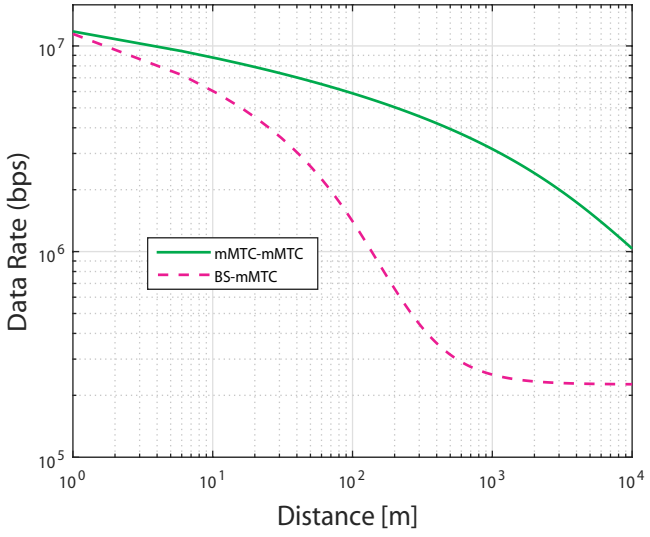

FIGURE 12. Data rate versus distance for mMTC communications, using optimal transmission power (unconstrained optimization) in THz band.

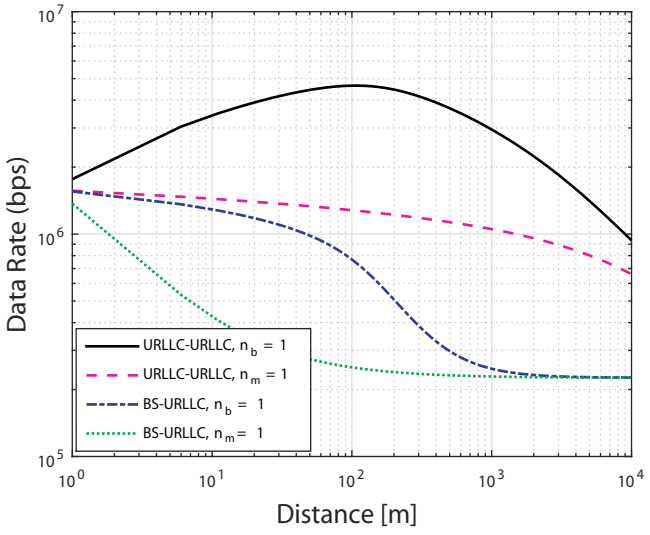

FIGURE 13. Data Rate versus distance for URLLC communications, using optimal transmission power (unconstrained optimization) in THz band.

is 36.55 dBm for mMTC, which is 2.7% lower than optimum power 37.57 dBm required for best case URLLC ($n_b = 1$) and 15.9% lower than optimal power 43.45 dBm required for worst case URLLC ($n_m = 1$). For B2M, at distance of 500 m, optimum power required for mMTC is 57.23 dBm, 2.7% lower than that required for best case URLLC ($n_b = 1$) at 58.82 dBm and 27.89% lower than worst case URLLC ($n_m = 1$) at 79.36 dBm.

Figure 12 shows the data rate vs distance for M2M and B2M mMTC, showing how the data rate decreases with distance between the communicating devices. Figure 13 shows the reducing trend of data rate with distance for each of the URLLC link (note that the initial increase for the M2M URLLC link is due to the decreasing effects on its interference, which enhanced the data rate performance till a certain distance). For M2M, at distance of 100 m the data rate is 5.870×10^6 bps for mMTC, which is 1.3 times higher than data rate, 4.649×10^6 bps, for best case URLLC ($n_b = 1$) and 4.6 times higher than data rate, 1.284×10^6 bps, for worst case URLLC ($n_m = 1$). For B2M, at distance of 500 m, data rate for mMTC is 3.15×10^5 bps, 5.56% higher than that of best case URLLC at 2.975×10^5 bps and 26% higher than worst case URLLC at 2.317×10^5 bps.

Figure 14 shows the plot of energy efficiency versus distance for M2M and B2M mMTC links, while the corresponding curves for URLLC links are shown in Fig. 15. For M2M, at distance of 100 m the energy efficiency is 5.616×10^4 bps/W for mMTC, which is 21.69% higher than corresponding energy efficiency of 4.398×10^4 bps/W for best case URLLC ($n_b = 1$). For B2M, at distance of 500 m, energy efficiency for mMTC is 501.3 bps/W, 1.5 times higher than that achieved for best case URLLC at 345.0 bps/W.

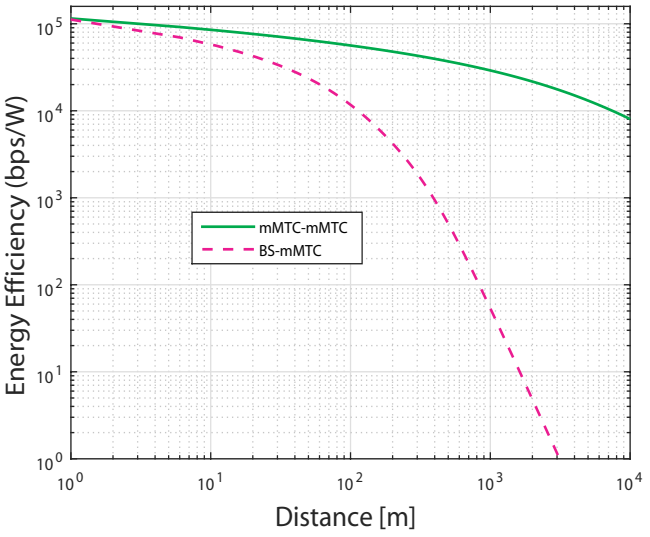

FIGURE 14. Energy efficiency versus distance for mMTC communication with optimal transmission power (unconstrained optimization) in THz band.

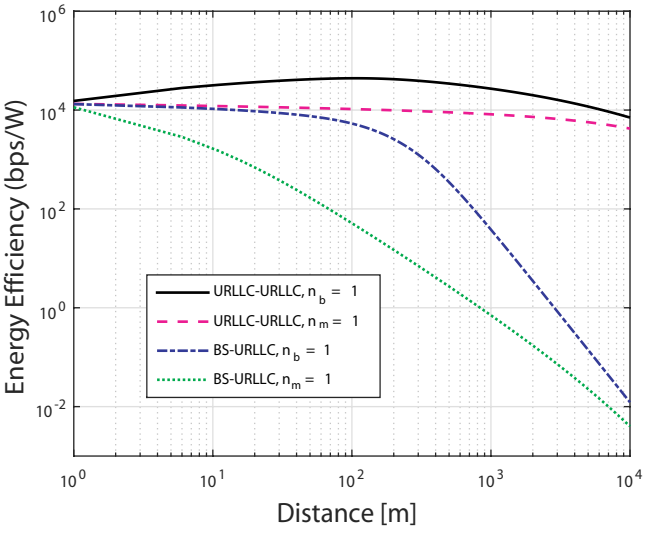

FIGURE 15. Energy efficiency versus distance for URLLC communication with optimal transmission power (unconstrained optimization) in THz band.

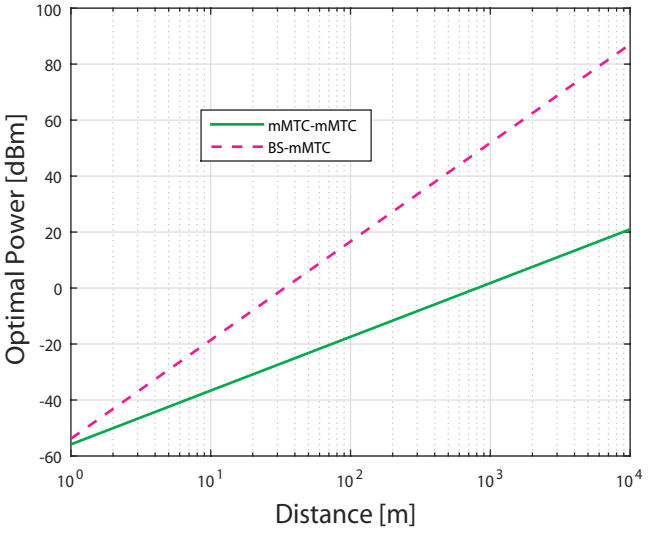

FIGURE 16. Optimal transmission power required versus distance for mMTC communication links (constrained optimization) in THz band.

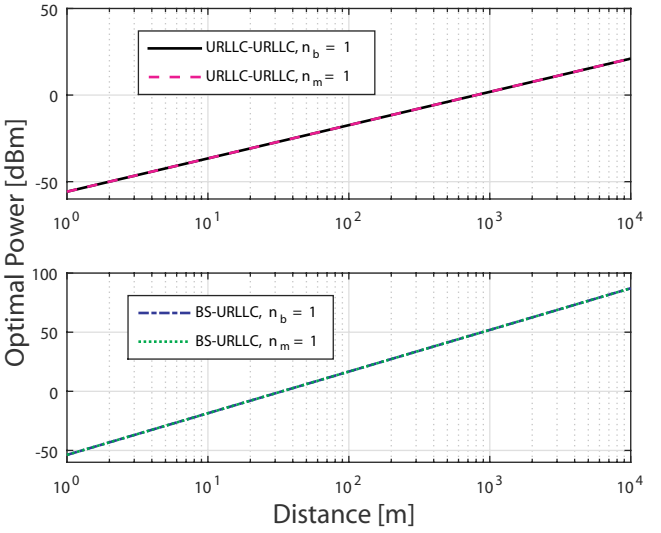

FIGURE 17. Optimal transmission power required versus distance for URLLC communication links (constrained optimization) in THz band.

C. SIMULATIONS AFTER CONSTRAINED OPTIMIZATION

The plots in Figs. 16-19, for constrained optimization, have been simulated using the equation (19), where $R_{th} = 10^5$, and then substituting into equations (11), (12) and (14) for data rate and energy efficiency.

The plots in Figs. 16 and 17, show the trends of optimal transmission power against the distance. With increasing distance between the devices, the path loss and hence the required transmission power increases. At a distance of 100 m the optimal power required is -17.34 dBm for M2M mMTC, lower than optimal power -17.28 dBm required for M2M URLLC. As for B2M, considering the point $d = 500$ m, the optimum power necessary for mMTC is 41.29 dBm, very close to that needed for URLLC at 41.35 dBm.

In Figs. 18 and 19 the plot of energy efficiency versus distance for mMTC and URLLC communication links. Regarding the M2M links, comparing at the distance of 100 m, the energy efficiency obtained is 1000 bps/W for mMTC, the same as 1000 bps/W obtained for M2M URLLC. As for B2M, considering distance of 500 m, the energy efficiency for mMTC is 410.7 bps/W, 8.06% times than that of URLLC at 377.6 bps/W. For this optimization technique, the data rates of mMTC and URLLC links, are all constant (i.e., 10^5) across the entire range of distance. This is because, transmission power increases with an increase in distance, which in turn improves the path loss. Therefore, the channel quality also improves.

V. CONCLUSION

To conclude, in this paper, an application of NOMA for MTC systems in the lower THz band was shown. A system model was presented and equations for the data rate, energy efficiency and optimal transmission power for its different communication links were provided. The performance of

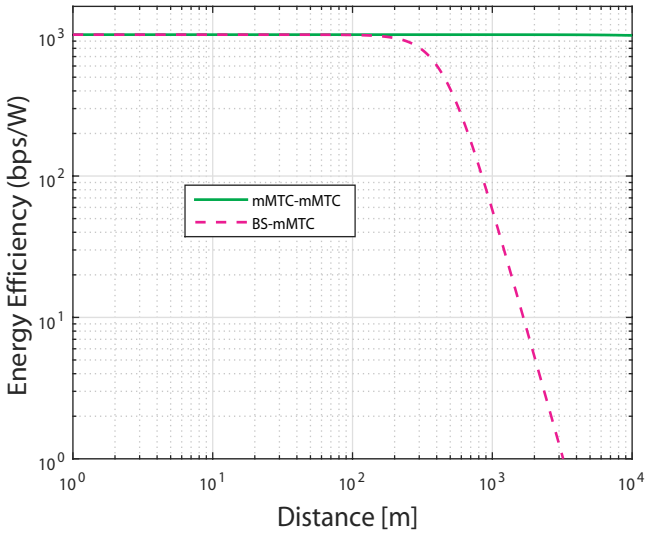

FIGURE 18. Energy efficiency versus distance for mMTC communication with optimal transmission power (constrained optimization) in THz band.

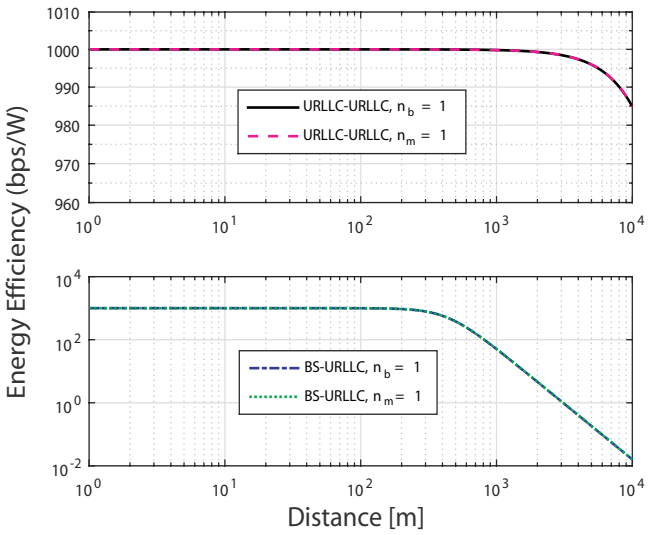

FIGURE 19. Energy efficiency versus distance for URLLC communication with optimal transmission power (constrained optimization) in THz band.

TABLE 3. Comparison between energy efficiency after unconstrained and constrained optimization.

Distance (m)	Communication link	Optimization I: Energy efficiency (no constraints) (bps/W)	Optimization II: Energy efficiency (with constraints) (bps/W)	Performance improvement / drop compared
100	mMTC-mMTC	5.616×10^4	1000	Optimization I > Optimization II (98.22% Drop)
100	URLLC-URLLC ($n_b = 1$)	4.398×10^4	1000	Optimization I > Optimization II (97.73% Drop)
100	URLLC-URLLC ($n_m = 1$)	1.048×10^4	1000	Optimization I > Optimization II (90.46% Drop)
500	BS-mMTC	501.3	410.7	Optimization I > Optimization II (18.07% Drop)
500	BS-URLLC ($n_b = 1$)	345.0	377.6	Optimization II > Optimization I (8.63% Improvement)
500	BS-URLLC ($n_m = 1$)	2.683	377.6	Optimization II > Optimization I (99.29% Improvement)

the model in terms of data rate, optimal transmission power and energy efficiency was evaluated and the plots from simulations were given. The optimization of the transmission power for maximum energy efficiency was derived via unconstrained and constrained optimization. Based on the trends of the plots and the numerical results as shown in Table 3, the following points are to be noted:

1) Implementing the proposed NOMA based system model in the lower THz band frequencies attains better overall performance with respect to data rate and energy efficiency than in lower frequencies such as the mmWave band.
2) The channel gain characteristics were better for M2M than B2M, so M2M communications attained higher data rate over B2M communications. The higher data rate of M2M led to its higher energy efficiency over B2M.
3) Using unconstrained optimization method, the optimal transmission power that was derived led to higher energy efficiency for all M2M communications at 100 m and for the B2M mMTC communication at 500 m, than the transmission power derived using constrained optimization method. On the other hand, the energy efficiency attained using constrained optimization method, led to a higher energy efficiency for both cases of the B2M URLLC communications at 500 m.
4) Thus, the best performance with regard to energy efficiency of the system model presented in this paper can be achieved by utilizing an integral use of two different techniques for the two types of communication links: unconstrained optimization for M2M communications and constrained optimization for B2M communica-

tions.

Based on the results and the research done for this study, we observed the potential of the lower THz band to improve the data rate and energy efficiency of MTC systems. Operating in this band, in conjunction with power domain multiplexing of NOMA and subcarrier sharing over OFDMA, can provide accommodation to a much greater number of wireless devices. The optimization techniques have been useful in resolving the question of power allocation for the differently powered devices in NOMA. Because low powered devices too have been optimized for energy efficiency, we believe that our techniques have enabled the best use of communication resources in protecting signal quality. In future works, further enhancements of this paper's model can be made by incorporating other promising techniques such as transmit antenna selection [27] and energy harvesting [28].

.

APPENDIX A PROOF OF OPTIMAL TRANSMISSION POWER VIA UNCONSTRAINED OPTIMIZATION

Energy efficiency as given in equation (14) expanded is of the form:

$$EE = \frac{B \cdot \log_2\left(1+\frac{p_t|h|^2}{N_oB+I}\right)}{P_{idle}+p_t} = \frac{B}{\ln(2)} \cdot \frac{\ln\left(1+\frac{p_t|h|^2}{N_oB+I}\right)}{P_{idle}+p_t}. \quad \text{(A.1)}$$

Now we derive the equation (A.1) with respect to p_t. We get

$$\frac{d(EE)}{dp_t} = \frac{B}{\ln 2} \cdot \frac{\frac{(P_{idle}+p_t)\cdot|h|^2}{(N_oB+I)\cdot(1+\frac{p_t|h|^2}{N_oB+I})} - \ln(1+\frac{p_t|h|^2}{N_oB+I})}{(P_{idle}+p_t)^2}. \quad \text{(A.2)}$$

Equating (A.2) to zero and changing sides leads to the following equation:

$$\frac{(P_{idle}+p_t)\cdot|h|^2}{N_oB+I} = \left(1+\frac{p_t|h|^2}{N_oB+I}\right)\cdot\ln\left(1+\frac{p_t|h|^2}{N_oB+I}\right). \quad \text{(A.3)}$$

Now we consider

$$e^f = 1+\frac{p_t|h|^2}{N_oB+I}, \quad \text{(A.4)}$$

where f is a variable.

Changing sides, variable f can be expressed as:

$$f = \ln\left(1+\frac{p_t|h|^2}{N_oB+I}\right). \quad \text{(A.5)}$$

Plugging in equation (A.5) in equation (A.4), the following are produced:

$$\frac{P_{idle}\cdot|h|^2}{N_oB+I} + e^f - 1 = e^f\cdot\ln(e^f)$$
$$\Rightarrow \frac{P_{idle}\cdot|h|^2}{N_oB+I} - 1 = (f-1)\cdot e^f. \quad \text{(A.6)}$$

Multiplying both sides of by e^{-1}, we get:

$$e^{-1}\cdot\frac{P_{idle}\cdot|h|^2}{N_oB+I} - 1 = (f-1)\cdot e^{f-1}. \quad \text{(A.7)}$$

Using the inverse of Lambert function, the right and hence the left side of the equation (A.7) can be written as:

$$W\left[e^{-1}\cdot\frac{P_{idle}\cdot|h|^2}{N_oB+I} - 1\right] = f-1. \quad \text{(A.8)}$$

Equation (A.5) can be plugged into equation (A.8) to arrive at:

$$f = \ln\left(1+\frac{p_t|h|^2}{N_oB+I}\right) = 1+W\left[e^{-1}\cdot\frac{P_{idle}\cdot|h|^2}{N_oB+I} - 1\right]. \quad \text{(A.9)}$$

Finally, changing side yields the expression for optimal transmission power for maximum energy efficiency.

APPENDIX B PROOF OF OPTIMAL TRANSMISSION POWER VIA CONSTRAINED OPTIMIZATION

Based on equation (18), the Lagrangian expression [29] can be expressed as

$$\mathcal{L}(p_t) = p_t + \lambda_1\cdot(R_{th}-R) + \lambda_2\cdot(p_{th}-p_t), \quad \text{(B.1)}$$

where λ_1 and λ_2 are Lagrangian multipliers corresponding to constraints (18b) and (18c).

The Lagrangian is differentiated with respect to p_t, λ_1, λ_2 and $|h|^2$ and then equated to zero each time to get the following equations:

$$\frac{d\mathcal{L}}{dp_t} = -\lambda_2 - \frac{B\cdot|h|^2\cdot\lambda_1}{(I+N_oB)\cdot\ln(2)\cdot(1+\frac{|h|^2\cdot p_t}{I+N_oB})} + 1 = 0$$
$$\Rightarrow \lambda_2 = 1 - \frac{B\cdot|h|^2\cdot\lambda_1}{(I+N_oB)\cdot\ln(2)\cdot(1+\frac{|h|^2\cdot p_t}{I+N_oB})}. \quad \text{(B.2)}$$

$$\frac{d\mathcal{L}}{d|h|^2} = -\frac{B\cdot p_t\cdot\lambda_1}{(I+N_oB)\cdot\ln(2)\cdot(1+\frac{|h|^2\cdot p_t}{(I+N_oB)})} = 0$$
$$\Rightarrow \lambda_1 = 0. \quad \text{(B.3)}$$

$$\frac{d\mathcal{L}}{d\lambda_1} = R_{th} - \frac{B\cdot\ln(1+\frac{|h|^2\cdot p_t}{I+N_oB})}{\ln(2)} = 0$$
$$\Rightarrow R_{th} = \frac{B\cdot\ln(1+\frac{|h|^2\cdot p_t}{I+N_oB})}{\ln(2)}. \quad \text{(B.4)}$$

$$\frac{d\mathcal{L}}{d\lambda_2} = p_{th} - p_t = 0$$
$$\Rightarrow p_t = p_{th}. \quad \text{(B.5)}$$

From equation (B.4),

$$\ln(2)R_{th} = B \cdot \ln\left(1 + \frac{|h|^2 \cdot p_t}{I + N_o B}\right)$$
$$\Rightarrow \ln\left(1 + \frac{|h|^2 \cdot p_t}{I + N_o B}\right) = \frac{\ln(2)R_{th}}{B}$$
$$\Rightarrow 1 + \frac{|h|^2 \cdot p_t}{I + N_o B} = \exp\left(\frac{\ln(2)R_{th}}{B}\right)$$
$$\Rightarrow p_t = \frac{I + N_o B}{|h|^2}\left[\exp\left(\frac{\ln(2)R_{th}}{B}\right) - 1\right]. \quad \text{(B.6)}$$

Plugging the expression for λ_1 found in equation (B.3) into equation (B.2) evaluates λ_2 to $\lambda_2 = 1$. Finally, plugging in expressions for λ_1 and λ_2 into equation (B.1):

$$\mathcal{L}(p_t) = p_t + 0 \cdot (R_{th} - R) + 1 \cdot (p_{th} - p_t). \quad \text{(B.7)}$$

And thus, the Lagrangian expression is

$$\mathcal{L}(p_t) = p_{th} = p_t. \quad \text{(B.8)}$$

REFERENCES

[1] K. Schwab, The Fourth Industrial Revolution, Crown Publishing Group, New York, 2017.
[2] T. S. Rappaport, Y. Xing, O. Kanhere, S. Ju, A. Madanayake, S. Mandal, A. Alkhateeb, G. C. Trichopoulos, "Wireless communications and applications above 100 GHz: Opportunities and challenges for 6G and beyond," *IEEE Access*, vol. 7, pp. 78729-78757, 2019.
[3] H. Elayan, O. Amin, R. M. Shubair, M-S. Alouini, "Terahertz communication: The opportunities of wireless technology beyond 5G," in *Proc. International Conference on Advanced Communication Technologies and Networking (CommNet)*, 2018.
[4] V. Petrov, A. Pyattaev, D. Moltchanov, and Y. Koucheryavy, "Terahertz band communications: Applications, research challenges, and standardization activities," in *Proc. 8th International Congress on Ultra Modern Telecommunications and Control Systems and Workshops (ICUMT)*, Dec. 2016.
[5] Y. Saito, Y. Kishiyama, A. Benjebbour, T. Nakamura, A. Li, and K. Higuchi, "Non-orthogonal multiple access (NOMA) for cellular future radio access," in *Proc. of the IEEE 77th Vehicular Technology Conference (VTC'13)*, pp. 1-5, Dresden, Germany, June 2013.
[6] M. Vaezi and H. V. Poor, "NOMA: An information-theoretic perspective," in *Multiple Access Techniques for 5G Wireless Networks and Beyond*, Springer International Publishing, pp. 167-193, Aug. 2018.
[7] L. Feltrin, G. Tsoukaneri, M. Condoluci, C. Buratti, T. Mahmoodi, M. Dohler, and R. Verdone, "Narrowband IoT: A survey on downlink and uplink perspectives," *IEEE Wireless Communications*, vol. 26, no. 1, pp. 78-86, Feb. 2019.
[8] A. E. Mostafa, Y. Zhou, and V. W. Wong, "Connectivity maximization for narrowband IoT systems with NOMA," in *Proc. IEEE International Conference on Communications (ICC)*, 2017.
[9] H. Ji, S. Park, J. Yeo, Y. Kim, J. Lee, and B. Shim, "Ultra-reliable and low-latency communications in 5G downlink: Physical layer aspects," *IEEE Wireless Communications*, vol. 25, no. 3, pp. 124-130, 2018.
[10] Z. Chen, Z. Ding, P. Xu and X. Dai, "Optimal precoding for a QoS optimization problem in two-user MISO-NOMA downlink," *IEEE Communications Letters*, vol. 20, no. 6, pp. 1263-1266, June 2016.
[11] Z. Ding, X. Lei, G. K. Karagiannidis, R. Schober, J. Yuan, and V. K. Bhargava, "A survey on non-orthogonal multiple access for 5G networks: Research challenges and future trends," *IEEE Journal on Selected Areas in Communications*, vol. 35, no. 10, pp. 2181-2195, Jul. 2017.
[12] F. Fang, H. Zhang, J. Cheng, and V. C. Leung, "Energy efficiency of resource scheduling for non-orthogonal multiple access (NOMA) wireless network," in *Proc. IEEE International Conference on Communications (ICC)*, Jul. 2016.
[13] H. Zhang, F. Fang, J. Cheng, K. Long, W. Wang, and V. C. M. Leung, "Energy-efficient resource allocation in NOMA heterogeneous networks," *IEEE Wireless Communications*, vol. 25, no. 2, pp. 48-53, Apr. 2018.
[14] H. Zhang, B. Wang, C. Jiang, K. Long, A. Nallanathan, V. C. M. Leung, and H. V. Poor, "Energy efficient dynamic resource optimization in NOMA system," *IEEE Transactions on Wireless Communications*, vol. 17, no. 9, pp. 5671-5683, Jun. 2018.
[15] P. Wu, J. Zeng, X. Su, H. Gao and T. Lv, "On energy efficiency optimization in downlink MIMO-NOMA," in *Proc. IEEE International Conference on Communications (ICC)*, pp. 399-404, Jul. 2017.
[16] M. Zeng, A. Yadav, O. A. Dobre, G. I. Tsiropoulos and H. V. Poor, "Capacity comparison between MIMO-NOMA and MIMO-OMA with multiple users in a cluster," *IEEE Journal on Selected Areas in Communications*, vol. 35, no. 10, pp. 2413-2424, Oct. 2017.
[17] M. Zeng, A. Yadav, O. A. Dobre, G. I. Tsiropoulos and H. V. Poor, "On the sum rate of MIMO-NOMA and MIMO-OMA systems," *IEEE Wireless Communications Letters*, vol. 6, no. 4, pp. 534-537, Aug. 2017.
[18] S. M. R. Islam, M. Zeng, O. A. Dobre and K. Kwak, "Resource allocation for downlink NOMA systems: Key techniques and open issues," *IEEE Wireless Communications*, vol. 25, no. 2, pp. 40-47, April 2018.
[19] M. Chen, Y. Miao, Y. Hao and K. Hwang, "Narrow band internet of things," *IEEE Access*, vol. 5, pp. 20557-20577, 2017.
[20] 3GPP, TR 25.814 V7.1.0, Release 7, Technical Specification Group Radio Access Networks Physical layer aspects for evolved Universal Terrestrial Radio Access (UTRA), Sept. 2006.
[21] ITU-R report M.2135, Guidelines for evaluation of radio interface technologies for IMT-Advanced, 2008.
[22] H. Xing and S. Hakola, "The investigation of power control schemes for a device-to-device communication integrated into OFDMA cellular system," in *Proc. 21st Annual IEEE International Symposium on Personal, Indoor and Mobile Radio Communications*, pp. 1775-1780, 2010.
[23] G. Wu, C. Yang, S. Li, and G. Y. Li, "Recent advances in energy-efficient networks and their application in 5G systems," *IEEE Wireless Communication*, vol. 22, no. 2, pp. 145-151, Apr. 2015.
[24] M. R. Mili, L. Musavian, K. A. Hamdi and F. Marvasti, "How to increase energy efficiency in cognitive radio networks," *IEEE Transactions on Communications*, vol. 64, no. 5, pp. 1829-1843, May 2016.
[25] K. Miettinen, Nonlinear Multiobjective Optimization, Springer, 1999.
[26] M. R. Akdeniz, Y. Liu, M. K. Samimi, S. Sun, S. Rangan, T. S. Rappaport and E. Erkip, "Millimeter wave channel modeling and cellular capacity evaluation," *IEEE Journal on Selected Areas in Communications*, vol. 32, no. 6, pp. 1164-1179, June 2014.
[27] S. R. Sabuj and M. Hamamura, "Outage and energy-efficiency analysis of cognitive radio networks: A stochastic approach to transmit antenna selection," *Pervasive and Mobile Computing*, Elsevier, vol. 42, pp. 444-469, 2017.
[28] S. R. Sabuj and M. Hamamura, "Two-slope path-loss design of energy harvesting in random cognitive radio networks," *Computer Networks*, Elsevier, vol. 142, pp. 128-141, 2018.
[29] S. Boyd and L. Vandenberghe, Convex Optimization. Cambridge, UK: Cambridge University Press, 2004.

A M MUSA SHAKIB KHAN is currently a final semester student of Electrical and Electronic Engineering (EEE) at Brac University, Dhaka, Bangladesh. His concentration within EEE is in Communications and Computers.

His research interest lies in technologies that facilitate 5G wireless communication (and beyond) such as multiple-access techniques, multiple input multiple output systems and means of optimizing communication for maximum performance and efficiency. He also studies software and hardware architectures of embedded systems, such as those constituting the Internet of things or having biomedical applications.

Mr. Khan has been awarded merit and performance scholarships at Brac University and was also a recipient of scholarship at McGill University, where he had previously studied for a number of semesters.

SAIFUR RAHMAN SABUJ (M'16) was born in Bangladesh in 1985. He received a B. Sc in Electrical, Electronic and Communication Engineering from Dhaka University, Bangladesh in 2007, an M. Sc Engineering in the Institute of Information and Communication Technology, Bangladesh University of Engineering and Technology, Bangladesh in 2011, and a Ph.D. degree in the Graduate School of Engineering, Kochi University of Technology, Japan in 2017.

From 2008 to 2013, he was a faculty member of Green University of Bangladesh, Metropolitan University, Sylhet and Bangladesh University. He has been in the position of an Assistant Professor in the department of Electrical and Electronic Engineering at Brac University, Bangladesh, since September 2017. He is currently working with Electronics and Control Engineering Department as a Postdoctoral Research Fellow at Hanbat National University, South Korea. His research interests include MIMO-OFDM/NOMA, Cooperative Communication, Cognitive Radio, Internet of things, and Machine-to-machine for wireless communications.

MASANORI HAMAMURA (M'00) received his B.S., M.S. and Ph.D. degrees in electrical engineering from Nagaoka University of Technology, Nagaoka, Japan, in 1993, 1995 and 1998, respectively. From 1998 to 2000, he was a Research Fellow of the Japan Society for the Promotion of Science.

Since 2000, he has been with the Department of Information Systems Engineering at Kochi University of Technology, Kochi, Japan, where he is now a Professor. From 1998 to 1999, he was a visiting researcher at Centre for Telecommunications Research, King's College London, United Kingdom, where he worked on adaptive signal processing for mobile systems. His current research interests are in the areas of signal design, wireless communications and signal processing.